

Elucidating the Mechanism of Uranium Mediated Diazene N=N Bond Cleavage

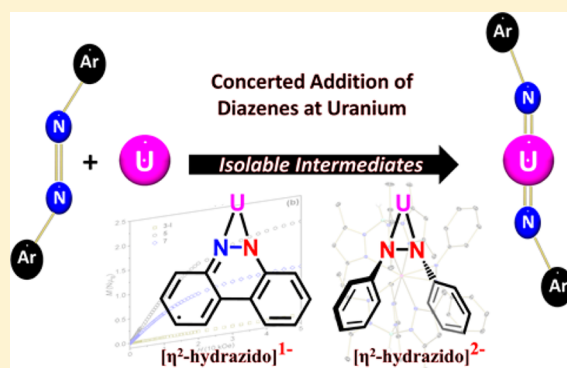
John J. Kiernicki,[†] Robert F. Higgins,[‡] Steven J. Kraft,[†] Matthias Zeller,[†] Matthew P. Shores,[‡] and Suzanne C. Bart^{*,†}

[†]H.C. Brown Laboratory, Department of Chemistry, Purdue University, West Lafayette, Indiana 47906, United States

[‡]Department of Chemistry, Colorado State University, Fort Collins, Colorado 80523, United States

S Supporting Information

ABSTRACT: Investigation into the reactivity of reduced uranium species toward diazenes has revealed key intermediates in the four-electron cleavage of azobenzene. Trivalent $\text{Tp}^*_2\text{U}(\text{CH}_2\text{Ph})$ (**1a**) (Tp^* = hydrotris(3,5-dimethylpyrazolyl)borate) and $\text{Tp}^*_2\text{U}(2,2'\text{-bpy})$ (**1b**) both perform the two-electron reduction of diazenes affording η^2 -hydrazido complexes $\text{Tp}^*_2\text{U}(\text{AzBz})$ (**2-AzBz**) (AzBz = azobenzene) and $\text{Tp}^*_2\text{U}(\text{BCC})$ (**2-BCC**) (BCC = benzo[*c*]cinnoline) in contrast to precursors of the bis(Cp^*) (Cp^* = 1,2,3,4,5-pentamethylcyclopentadienide) ligand framework. The four-electron cleavage of diazenes to give *trans*-bis(imido) species was possible by using $\text{Cp}^*\text{U}(\text{MesPDI}^{\text{Me}})(\text{THF})$ (**3**) ($\text{MesPDI}^{\text{Me}}$ = 2,6-((Mes)N=CMe)₂-C₅H₃N, Mes = 2,4,6-trimethylphenyl), which is supported by a highly reduced trianionic chelate that undergoes electron transfer. This proceeds via concerted addition at a single uranium center supported by both a crossover experiment and through addition of an asymmetrically substituted diazene, Ph-N=N-Tol. Further investigation of **3** and its substituted analogue, $\text{Cp}^*\text{U}(\text{tBu-MesPDI}^{\text{Me}})(\text{THF})$ (**3-tBu**) ($\text{tBu-MesPDI}^{\text{Me}}$ = 2,6-((Mes)N=CMe)₂-*p*-C(CH₃)₃-C₅H₂N), with benzo[*c*]cinnoline, revealed that the four-electron cleavage occurs first by a single electron reduction of the diazene with the redox chemistry performed solely at the redox-active pyridine(diimine) to form dimeric [$\text{Cp}^*\text{U}(\text{BCC})(\text{MesHPDI}^{\text{Me}})$]₂ (**5**) and $\text{Cp}^*\text{U}(\text{BCC})(\text{tBu-MesPDI}^{\text{Me}})$ (**6**). While a transient pyridine(diimine) triplet diradical in the formation of **5** results in H atom abstraction and *p*-pyridine coupling, the *tert*-butyl moiety in **6** allows for electronic rearrangement to occur, precluding deleterious pyridine-radical coupling. The monomeric analogue of **5**, $\text{Cp}^*\text{U}(\text{BCC})(\text{MesHPDI}^{\text{Me}})$ (**7**), was synthesized via salt metathesis from $\text{Cp}^*\text{UI}(\text{MesPDI}^{\text{Me}})$ (**3-I**). All complexes have been characterized by ¹H NMR and electronic absorption spectroscopies, X-ray diffraction, and, where pertinent, EPR spectroscopy. Further, the electronic structures of **3-I**, **5**, and **7** have been investigated by SQUID magnetometry.



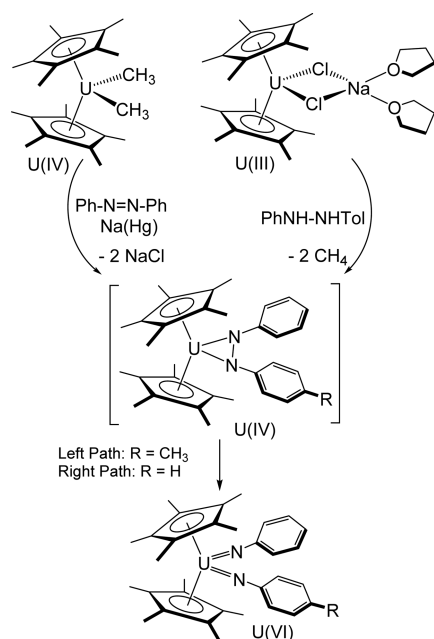
INTRODUCTION

As a fundamental step in the conversion of dinitrogen to ammonia, cleavage of strong N–N bonds has been widely studied for both industrial and biological applications.¹ Transition metals have enjoyed widespread use for this goal, as their ability to backbond into the low lying π^* orbitals of dinitrogen results in activation, and in some instances, complete scission.^{2,3} While the actinides are not known to engage in backbonding to the same extent as transition metals, the large size and highly reducing nature of these elements, and more specifically uranium, make them viable candidates to perform N–N cleavage.⁴ Uranium is also advantageous due to its available oxidation states, such that cleavage of a diazene (often a model for dinitrogen) by an electron-rich center could be achieved to form the corresponding high valent uranium bis(imido) species. Such is the case in the synthesis of the uranium(VI) *cis*-bis(imido), $\text{Cp}^*_2\text{U}(\text{NPh})_2$. Although first generated by Burns and co-workers via organoazide oxidation of the uranium(IV) imido, $[\text{Li}(\text{TMEDA})][(\text{Cp}^*_2\text{U}(\text{NPh})\text{Cl})]_5$

later studies showed that $\text{Cp}^*_2\text{U}(\text{NPh})_2$ can also be generated by azobenzene cleavage by a variety of low valent starting materials, which act as divalent^{6,7} “[Cp^*_2U]” synthons, including Cp^*_3U ,⁸ $\text{Cp}^*_2\text{U}(\eta^6:\eta^6\text{-C}_6\text{H}_6)\text{UCp}^*_2$,⁹ $[\text{Cp}^*_2\text{U}][(\mu\text{-Ph})_2\text{BPh}_2]$,¹⁰ $\text{Cp}^*\text{U}[\mu\text{-C}_5\text{Me}_3(\text{CH}_2)_2](\mu\text{-H})_2\text{UCp}^*_2$,¹¹ and $\text{Cp}^*_2\text{UCl}(\text{NaCl})/\text{Na}(\text{Hg})$ (Scheme 1).¹² Mechanistic support for the N–N cleavage came from generation of a fleeting side-on bound uranium(IV) hydrazido intermediate, $\text{Cp}^*_2\text{U}(\eta^2\text{-N}_2\text{Ph}_2)$,¹² derived from protonation of $\text{Cp}^*_2\text{U}(\text{Me})_2$ by PhNHNHPh , which proceeds to the *cis*-bis(imido) product.¹³ Mechanistic experiments employing the mixed hydrazine, PhNHNH-p-Tol , suggest a concerted process, as $\text{Cp}^*_2\text{U}(\text{NPh})(\text{N-p-Tol})$ is isolated as the sole product.¹³ This pioneering work sparked subsequent studies examining the formation of uranium complexes featuring side-on, η^2 -

Received: August 10, 2016

Scheme 1. Examples of *cis*-Bis(imido) Formation by Burns and Coworkers with Proposed η^2 -Hydrazido Intermediates



hydrazido ligands,^{14,15} lending additional support to the proposed “Cp*₂U(η^2 -N₂Ph₂)” intermediate.

In related work by our laboratory, we have studied uranium(IV) hydrazido species supported by the hydrotris-(3,5-dimethylpyrazolyl)borate ligand, namely, Tp*₂U(N₂CPh₂) and Tp*₂U(N₂CHSiMe₃), which were constructed via diazoalkane reduction.¹⁶ Because Tp* is more sterically demanding than Cp*, these derivatives were found as the end-on, η^1 -hydrazido species at room temperature in solution. Fortunately, evidence for a side-on, η^2 -hydrazido species was obtained for Tp*₂U(N₂CPh₂), both in solution below -5°C and from X-ray diffraction analysis of crystals grown at -35°C . Interestingly, in contrast to what was noted by Burns, no N–N cleavage was ever observed, despite the reduced N–N bond distance.

In our hands, N–N bond cleavage has been observed by the electron-rich uranium starting materials, Cp*U(^{Mes}PDI^{Me})(THF) (**3**)¹⁷ and Cp*U(^tBu-^{Mes}PDI^{Me})(THF) (**3-^tBu**),¹⁸ which bear triply anionic redox-active pyridine(diimine) ligands. The uranium and ligand electrons work cooperatively to reduce 1 equiv of azobenzene (PhN=NPh), affording the corresponding uranium(V) *trans*-bis(imido) species, Cp*U-(NPh)₂(^{Mes}PDI^{Me}).^{17,19} In these cases, all three ligand electrons as well as one uranium electron have been oxidized. Interestingly, substitution of PhN=NPh with *para*-methyl groups to generate TolN=NTol does not preclude reactivity, even with the higher reduction potential for the tolyl derivative. Instead, the resulting uranium *trans*-bis(imido) species have different electronic structures than their phenyl analogues. Both Cp*U(N^tol)₂(^{Mes}PDI^{Me})^{17,19} and Cp*U-(N^tol)₂(^tBu-^{Mes}PDI^{Me}) have spectroscopic and structural features that are consistent with uranium(VI) centers supported by monoanionic [^{Mes}PDI^{Me}]¹⁻ ligands, where both the uranium and ^{Mes}PDI^{Me} ligand have been oxidized by two electrons.¹⁹

On the basis of these preliminary results, we aimed to explore the reductive capabilities of uranium(III) and (IV) complexes toward N–N bonds, and also to further probe the stability of uranium(IV) hydrazido species, which are often invoked as

intermediates in the four-electron cleavage of azobenzene. First, the synthesis and characterization of elusive uranium(IV) hydrazido species are facilitated by the sterically bulky Tp* supporting ligands. Second, concomitant studies focused on understanding the reductive capabilities of **3** and **3-^tBu** toward diazenes for the formation of uranium(IV) hydrazido complexes are discussed. Finally, the possibility for a second two-electron reduction of diazene to form uranium *trans*-bis(imido) species is examined, and mechanistic support to demonstrate concerted addition at a monomeric uranium compound is provided. Full spectroscopic and structural characterization of all compounds is reported.

EXPERIMENTAL SECTION

All air- and moisture-sensitive manipulations were performed using standard Schlenk techniques or in an MBraun inert atmosphere drybox with an atmosphere of purified nitrogen. The MBraun drybox was equipped with a cold well designed for freezing samples in liquid nitrogen as well as two -35°C freezers for cooling samples and crystallizations. Solvents for sensitive manipulations were dried and deoxygenated using literature procedures with a Seca solvent purification system.²⁰ Benzene-*d*₆ was purchased from Cambridge Isotope Laboratories, dried with molecular sieves and sodium, and degassed by three freeze–pump–thaw cycles. Tp*₂U(CH₂Ph) (**1a**),²¹ Tp*₂U(2,2'-bpy) (**1b**),²² Cp*U(^{Mes}PDI^{Me})(THF) (**3**),¹⁷ Cp*U-(^tBu-^{Mes}PDI^{Me})(THF) (**3-^tBu**),¹⁸ Cp*UI(^{Mes}PDI^{Me}) (**3-I**),²³ 1,2-di-*p*-tolyl diazene (Tol-N=N-Tol),²⁴ and 1-phenyl-2-(*p*-tolyl) diazene (Ph-N=N-Tol)²⁵ were prepared according to literature procedures. Benzo[*c*]cinnoline (VWR) and azobenzene (Sigma-Aldrich) were used as received. Synthetic procedures for the synthesis of **2-AzBz** and **2-BCC** from **1b** are provided in the Supporting Information.

¹H NMR spectra were recorded on a Varian Inova 300 spectrometer operating at 299.992 MHz. All chemical shifts are reported relative to the peak for SiMe₄, using ¹H (residual) chemical shifts of the solvent as a secondary standard. The spectra for paramagnetic molecules were obtained by using an acquisition time of 0.5 s; thus, the peak widths reported have an error of ± 2 Hz. For paramagnetic molecules, the ¹H NMR data are reported with the chemical shift, followed by the peak width at half height in Hertz, the integration value, and, where possible, the peak assignment. Elemental analyses were performed by either Complete Analysis Laboratories, Inc. (Parsippany, NJ) or Galbraith Laboratories, Inc. (Knoxville, TN). Electronic absorption measurements were recorded at 294 K in sealed 1 cm quartz cuvettes with a Jasco V-6700 spectrophotometer.

The LUMO depiction of benzo[*c*]cinnoline (Scheme 2) was generated using GaussView 5.²⁶ EPR samples of **5**–**7** were prepared in sealed J-Young EPR tubes, and data were reproduced over a minimum of two samples in toluene. The EPR sample of K(benzo[*c*]cinnoline) was prepared by addition of potassium graphite (0.081 mmol) to a -35°C THF solution (2 mL) of benzo[*c*]cinnoline (0.089 mmol), filtration, and dilution with toluene.

Single crystals of Tp*₂U(BCC) (**2-BCC**), Cp*U(NPh)(NTol)-(^{Mes}PDI^{Me}) (**4-Ph/Tol**), [Cp*U(BCC)(^{Mes}PDI^{Me})₂] (**5**), Cp*U-(BCC)(^tBu-^{Mes}PDI^{Me}) (**6**), and Cp*U(BCC)(^{Mes}PDI^{Me}) (**7**) suitable for X-ray diffraction were coated with poly(isobutylene) oil in a glovebox and quickly transferred to the goniometer head of a Nonius KappaCCD diffractometer at low temperature (see CIF) equipped with a graphite crystal, incident beam monochromator using Mo *K* α radiation ($\lambda = 0.71073 \text{ \AA}$). Data were collected using the Nonius Collect software, processed using HKL3000, and corrected for absorption and scaled using Scalepack. Crystals of Tp*₂U([η^2 -N,N'-(C₆H₅N–NC₆H₅)] (**2-AzBz**) were transferred to the goniometer head of a Bruker APEX II CCD diffractometer at 100 K using monochromatic Mo *K* α radiation ($\lambda = 0.71073 \text{ \AA}$) with the ω scan technique. Data for **2-AzBz** were collected, and its unit cell was determined; the data were integrated and corrected for absorption and other systematic errors using the Apex2 suite of programs.²⁷ The space groups were assigned, and the structure was solved by direct methods

using XPREP within the SHELXTL suite of programs^{28,29} and refined by full matrix least-squares against F^2 with all reflections using SHELXL 2014³⁰ and the graphical interface SHELXLX.³¹

All voltammetric data were obtained under inert atmosphere conditions using external electrical ports of the MBraun drybox using a Gamry Instruments Interface 1000 model potentiostat with the Gamry Instruments Laboratory software. Data were acquired in acetonitrile with 0.1 M $[\text{Bu}_4\text{N}][\text{PF}_6]$ as the supporting electrolyte without internal resistance corrections. Solutions were measured in 4 dram cells, consisting of a 3 mm glassy carbon working electrode, a Pt wire counter electrode, and a Ag wire quasireference electrode. Potential corrections were performed at the end of the experiment using the $\text{Fc}^{0/+}$ couple as the internal standard.

Magnetic susceptibility data were collected on at least two independently prepared solid samples for 3-I, 5, and 7 using a Quantum Design MPMS XL SQUID magnetometer. Plots of susceptibility data for each species can be found in the Supporting Information (Figures S13–S15). All sample preparations were performed inside a dinitrogen-filled glovebox (MBraun Labmaster 130). Powdered microcrystalline samples were loaded into polyethylene bags, sealed in the glovebox, inserted into a straw, and transported to the magnetometer under nitrogen. Ferromagnetic impurities were checked through a variable field analysis (0 to 10 kOe) of the magnetization at 100 K: curvature in the M versus H plot between 0 and ~ 2000 Oe (Figures S5–S10) indicates the presence of ferromagnetic impurities. When this behavior was observed, susceptibility data were collected at magnetic fields where the field dependence is linear (5000 Oe for these compounds). Magnetic susceptibility data were collected at temperatures ranging from 2 (4 K for compound 7) to 300 K. Susceptibility data reproducibility was assessed through measurements on two different batches for compounds 3-I, 5, and 7 (Figures S13–S15). The maximum difference observed was $0.10 \text{ cm}^3 \text{ K/mol}$ at 225 K for complex 3-I. Magnetization measurements were collected at 1.8 K at applied fields ranging from 0 to 50 kOe. Data were corrected for the diamagnetic contributions of the sample holder and bag by subtracting empty containers; corrections for the sample were calculated from Pascal's constants.³²

Synthesis of $\text{Tp}^*_2\text{U}[\eta^2\text{-N,N'}\text{-(C}_6\text{H}_5\text{N-NC}_6\text{H}_5)]$ (2-AzBz) from 1a. A 20 mL scintillation vial was charged with $\text{Tp}^*_2\text{U}(\text{CH}_2\text{Ph})$ (1a) (0.140 g, 0.208 mmol) and 10 mL of THF and chilled to -35 °C. While the reaction mixture was stirred, azobenzene (0.038 g, 0.208 mmol) was added resulting in a gradual color change from dark green to brown over a few minutes. After 1 h, volatiles were removed *in vacuo*, and the crude mixture was washed with *n*-pentane to afford yellow-brown powder (0.141 g, 0.141 mmol, 92% yield) assigned as $\text{Tp}^*_2\text{U}[\eta^2\text{-N,N'}\text{-(C}_6\text{H}_5\text{N-NC}_6\text{H}_5)]$ (2-AzBz). Single, X-ray quality crystals were obtained from a concentrated THF solution stored at -35 °C. Anal. for $\text{C}_{42}\text{H}_{54}\text{N}_{14}\text{B}_2\text{U}$ Calcd: C, 49.72; H, 5.36; N, 19.33. Found: C, 49.12; H, 5.54; N, 19.00. $^1\text{H NMR}$ (C_6D_6 , 25 °C): $\delta = -57.25$ (9, 6H, $\text{Tp}^*\text{-CH}_3$), -30.00 (18, 2H, ArH), -18.69 (5, 6H, $\text{Tp}^*\text{-CH}_3$), -12.44 (3, 2H, ArH), -11.95 (5, 6H, $\text{Tp}^*\text{-CH}_3$), -10.62 (34, 2H, ArH), -4.19 (4, 2H, ArH), -1.02 (8, 6H, $\text{Tp}^*\text{-CH}_3$), 0.00 (4, 6H, $\text{Tp}^*\text{-CH}_3$), 10.09 (t, $J = 7$, 2H, Ph-*p*-CH), 32.77 (4, 2H, ArH), 33.26 (33, 2H, ArH), 66.50 (12, 6H, $\text{Tp}^*\text{-CH}_3$), 84.04 (35, 2H, ArH). $^{11}\text{B NMR}$ (C_6D_6 , 25 °C): $\delta = -90.32$. IR (KBr salt plate) $\nu = 2552$, 2521 cm^{-1} (B–H).

Synthesis of $\text{Tp}^*_2\text{U}(\text{BCC})$ (2-BCC) from 1a. A 20 mL scintillation vial was charged with $\text{Tp}^*_2\text{U}(2,2'\text{-bpy})$ (1) (0.100 g, 0.110 mmol) and 5 mL of THF and chilled to -35 °C. While the reaction mixture was stirred, benzo[*c*]cinnoline (0.020 g, 0.111 mmol) was added resulting in a rapid color change from dark green to red-brown. After 1 h, volatiles were removed *in vacuo*. The crude mixture was washed with cold *n*-pentane to afford dark powder (0.085 g, 0.085 mmol, 77%) assigned as $\text{Tp}^*_2\text{U}(\text{BCC})$ (2-BCC). Single, X-ray quality crystals were obtained from a concentrated diethyl ether/THF (1:3) solution stored at -35 °C. Anal. for $\text{C}_{42}\text{H}_{52}\text{N}_{14}\text{B}_2\text{U}$ Calcd: C, 49.82; H, 5.18; N, 19.37. Found: C, 49.07; H, 4.81; N, 18.03. $^1\text{H NMR}$ (C_6D_6 , 25 °C): $\delta = -28.52$ (8, 6H, $\text{Tp}^*\text{-CH}_3$), -20.48 (20, 2H, BCC-ArH), -17.94 (18, 2H, BCC-ArH), -14.58 (154, 2H, BH), -11.69 (3, 6H, $\text{Tp}^*\text{-CH}_3$), -4.13 (3, 6H, $\text{Tp}^*\text{-CH}_3$), -3.28 (3, 2H, $\text{Tp}^*\text{-CH}$),

0.24 (3, 6H, $\text{Tp}^*\text{-CH}_3$), 0.72 (4, 2H, $\text{Tp}^*\text{-CH}$), 5.04 (6, 6H, $\text{Tp}^*\text{-CH}_3$), 20.88 (3, 2H, $\text{Tp}^*\text{-CH}$), 22.24 (t, $J = 5$, 2H, BCC-ArH), 32.89 (d, $J = 8$, 2H, BCC-ArH), 33.72 (8, 6H, $\text{Tp}^*\text{-CH}_3$). $^{11}\text{B NMR}$ (C_6D_6 , 25 °C): $\delta = -52.40$. IR (KBr salt plate) $\nu = 2556$, 2526 cm^{-1} (B–H).

Synthesis of $\text{Cp}^*\text{U}(\text{NPh})(\text{NTol})^{(\text{MesPDI}^{\text{Me}})}$ (4-Ph/Tol). A 20 mL scintillation vial was charged with $\text{Cp}^*\text{U}^{(\text{MesPDI}^{\text{Me}})}(\text{THF})$ (3) (0.145 g, 0.172 mmol) and 5 mL of toluene. While the reaction mixture was stirred, Ph-N=N-Tol (0.034 g, 0.173 mmol) was added and stirred for 5 min. After removal of volatiles *in vacuo*, the product was washed with cold *n*-pentane and dried to afford brown powder (0.128 g, 0.132 mmol, 77%) assigned as $\text{Cp}^*\text{U}(\text{NPh})(\text{NTol})^{(\text{MesPDI}^{\text{Me}})}$ (4-Ph/Tol). Single, X-ray quality crystals were obtained from a concentrated diethyl ether solution at -35 °C. Anal. for $\text{C}_{50}\text{H}_{58}\text{N}_5\text{U}$ Calcd: C, 62.10; H, 6.05; N, 7.24. Found: C, 62.62; H, 6.42; N, 7.48. $^1\text{H NMR}$ (C_6D_6 , 25 °C): $\delta = -10.34$ (60, 6H, CH_3), -5.23 (60, 2H, ArH), -4.36 (60, 1H, ArH), -3.64 (22, 15H, Cp^*), 0.07 (30, 2H, ArH), 0.53 (65, 2H, CH_3), 0.71 (47, 2H, CH_3), 2.76 (46, 2H, ArH), 6.32 (17, 2H, ArH), 8.54 (290, 6H, CH_3), 10.95 (23, 2H, ArH), 12.58 (70, 2H, ArH), 14.87 (59, 3H, Tol- CH_3), 22.68 (112, 6H, CH_3), 28.63 (393, 6H, CH_3).

Crossover Experiment between $\text{Cp}^*\text{U}^{(\text{MesPDI}^{\text{Me}})}(\text{THF})$, Ph-N=N-Ph and Tol-N=N-Tol. A 20 mL scintillation vial was charged with $\text{Cp}^*\text{U}^{(\text{MesPDI}^{\text{Me}})}(\text{THF})$ (1) (0.050 g, 0.059 mmol) and 5 mL of toluene. In a separate vial, Ph-N=N-Ph (0.005 g, 0.027 mmol) and Tol-N=N-Tol (0.006 g, 0.029 mmol) were dissolved in 3 mL of toluene and added dropwise to the first vial with stirring. After 15 min, volatiles were removed *in vacuo*. $^1\text{H NMR}$ analysis of the crude mixture revealed $\text{Cp}^*\text{U}(\text{NPh})_2^{(\text{MesPDI}^{\text{Me}})}$ (4-Ph) and $\text{Cp}^*\text{U}(\text{NTol})_2^{(\text{MesPDI}^{\text{Me}})}$ (4-Tol), as compared to authentic samples. Complex 4-Ph/Tol was not observed.

Synthesis of $[\text{Cp}^*\text{U}(\text{BCC})^{(\text{MesHPDI}^{\text{Me}})}]_2$ (5). A 20 mL scintillation vial was charged with $\text{Cp}^*\text{U}^{(\text{MesPDI}^{\text{Me}})}(\text{THF})$ (3) (0.125 g, 0.148 mmol) and 5 mL of toluene. While the reaction mixture was stirred, benzo[*c*]cinnoline (0.027 g, 0.150 mmol) was added and stirred for 15 min. After removal of volatiles *in vacuo*, the product was recrystallized from a concentrated *n*-pentane and dried to afford brown powder (0.105 g, 0.055 mmol, 74%) assigned as $[\text{Cp}^*\text{U}(\text{BCC})^{(\text{MesHPDI}^{\text{Me}})}]_2$ (5). Single, X-ray quality crystals were obtained from concentrated THF solution layered with *n*-pentane at -35 °C. Anal. for $\text{C}_{98}\text{H}_{110}\text{N}_{10}\text{U}_2$ Calcd: C, 61.82; H, 5.82; N, 7.36. Found: C, 61.63; H, 5.67; N, 7.51. $^1\text{H NMR}$ (C_6D_6 , 25 °C): $\delta = -211.62$ (249, 4H, BCC-ArH), -153.27 (240, 4H, BCC-ArH), -32.28 (70, 6H, CH_3), -20.24 (20, 6H, CH_3), -7.98 (11, 6H, CH_3), -0.98 (10, 2H, ArH), 0.06 (13, 6H, CH_3), 1.11 (20, 30H, Cp^*), 4.49 (9, 6H, CH_3), 4.76 (7, 6H, CH_3), 5.65 (9, 2H, ArH), 6.75 (10, 2H, ArH), 8.69 (16, 2H, ArH), 10.09 (24, 6H, CH_3), 12.57 (10, 2H, ArH), 18.79 (124, 6H, CH_3), 28.65 (24, 2H, ArH), 32.98 (28, 2H, ArH), 37.31 (32, 2H, ArH), 56.57 (240, 4H, BCC-ArH), 60.11 (480, 4H, BCC-ArH).

Synthesis of $\text{Cp}^*\text{U}(\text{BCC})^{(\text{tBu-MesPDI}^{\text{Me}})}$ (6). A 20 mL scintillation vial was charged with $\text{Cp}^*\text{U}^{(\text{tBu-MesPDI}^{\text{Me}})}(\text{THF})$ (3-Bu) (0.145 g, 0.161 mmol) and 5 mL of toluene. While the reaction mixture was stirred, benzo[*c*]cinnoline (0.029 g, 0.161 mmol) was added and stirred for 5 min. After removal of volatiles *in vacuo*, the product was recrystallized from a concentrated *n*-pentane solution to afford brown powder (0.105 g, 0.104 mmol, 65%) assigned as $\text{Cp}^*\text{U}(\text{BCC})^{(\text{tBu-MesPDI}^{\text{Me}})}$ (6). Single, X-ray quality crystals were obtained from a concentrated toluene/*n*-pentane solution (2:1) at -35 °C. Anal. for $\text{C}_{53}\text{H}_{62}\text{N}_5\text{U}$ Calcd: C, 63.21; H, 6.21; N, 6.95. Found: C, 62.94; H, 6.27; N, 7.10. $^1\text{H NMR}$ (C_6D_6 , 25 °C): $\delta = -138.23$ (t, $J = 7$, 2H, BCC 2,9-ArH), -112.48 (d, $J = 8$, 2H, BCC 4,7-ArH), -5.74 (d, $J = 23$, 1H, ArH), -4.09 (d, $J = 23$, 1H, ArH), -0.13 (6, 3H, CH_3), 0.64 (4, 9H, $\text{C}(\text{CH}_3)_3$), 0.66 (7, 3H, CH_3), 4.09 (6, 1H, ArH), 4.22 (4, 15H, Cp^*), 4.60 (4, 3H, CH_3), 6.82 (5, 3H, CH_3), 8.00 (17, 1H, ArH), 8.06 (4, 3H, CH_3), 12.38 (15, 3H, CH_3), 12.86 (14, 1H, ArH), 17.48 (9, 1H, ArH), 34.23 (d, $J = 7$, 2H, BCC 1,10-ArH), 36.18 (t, $J = 7$, 2H, BCC 3,8-ArH), 135.20 (20, 3H, CH_3), 181.81 (28, 3H, CH_3).

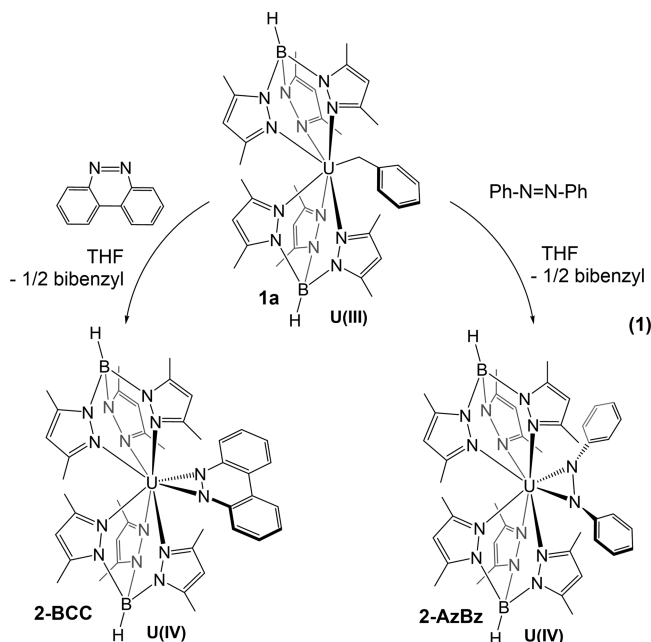
Synthesis of $\text{Cp}^*\text{U}(\text{BCC})^{(\text{MesPDI}^{\text{Me}})}$ (7). A 20 mL scintillation vial was charged with benzo[*c*]cinnoline (0.028 g, 0.155 mmol) and 5 mL of THF. While the reaction mixture was stirred, potassium graphite (0.021 g, 0.155 mmol) was added, resulting in an immediate color

change to vibrant green. This green solution was added dropwise to a vial containing $\text{Cp}^*\text{UI}(\text{MesPDI}^{\text{Me}})$ (0.139 g, 0.155 mmol) in THF (5 mL) resulting in immediate color change to dark brown. After 15 min, volatiles were removed *in vacuo*. The product was extracted into diethyl ether, filtered over Celite, and dried to afford brown powder (0.135 g, 0.142 mmol, 92%) assigned as $\text{Cp}^*\text{U}(\text{BCC})(\text{MesPDI}^{\text{Me}})$ (**7**). Single, X-ray quality crystals were obtained from a concentrated hexamethyldisiloxane/*n*-pentane (1:5) solution stored at -35°C . Anal. for $\text{C}_{49}\text{H}_{54}\text{N}_5\text{U}$ Calcd: C, 61.88; H, 5.72; N, 7.36. Found: C, 60.76; H, 6.06; N, 7.28. ^1H NMR (C_6D_6 , 25°C): $\delta = -216.46$ (66, 2H, BCC 2,9-ArH), -158.04 (45, 2H, BCC 4,7-ArH), -30.35 (19, 6H, CH_3), -3.17 (39, 6H, CH_3), -1.51 (62, 6H, CH_3), -0.79 (10, 2H, ArH), 1.95 (14, 15H, Cp^*), 2.66 (3, 6H, CH_3), 4.77 (6, 2H, ArH), 12.91 (81, 2H, *m*-pyr-CH), 15.38 (202, 1H, *p*-pyr-CH), 60.89 (16, 2H, BCC 1,10-ArH), 62.73 (16, 2H, BCC 3,8-ArH).

RESULTS AND DISCUSSION

Tp^* Uranium Derivatives. In order to probe the mechanistic proposal for formation of intermediate η^2 -hydrazido compounds shown in Scheme 1, we sought to generate isolable forms of these. Since Cp^* did not afford the steric protection to allow isolation of $\text{Cp}^*\text{U}(\eta^2\text{-N}_2\text{Ph}_2)$ as noted by Burns,¹² the analogous Tp^* ligand was utilized as its superior steric protection has been integral in the isolation of reactive species.³³ As both $\text{Tp}^*\text{U}(\text{CH}_2\text{Ph})$ (**1a**) and $\text{Tp}^*\text{U}(2,2'\text{-bpy})$ (**1b**) have been shown to behave as sources of " Tp^*U ",^{16,34–36} initial experiments were performed with these.

Addition of azobenzene to a chilled THF solution (-35°C) of **1a** resulted in a gradual color change from dark green to yellow-brown (eq 1). Analysis of the crude mixture by ^1H



NMR spectroscopy revealed the extrusion of bibenzyl, suggesting diazene reduction rather than U–C insertion. Following workup, the ^1H NMR spectrum of the product displayed 14 paramagnetically shifted resonances ranging from -57.25 to 84.04 ppm, precluding the assignment as a diamagnetic uranium(VI) bis(imido). Instead, the spectroscopic data are consistent with azobenzene reduction, leading to the assignment as $\text{Tp}^*\text{U}[\eta^2\text{-N,N}'\text{-(C}_6\text{H}_5\text{-N=N-C}_6\text{H}_5)]$ (**2-AzBz**) (eq 1, right). Characterization by infrared (B–H: $\nu = 2552, 2521\text{ cm}^{-1}$) and ^{11}B NMR spectroscopies (-90.32 ppm) confirmed retention of the Tp^* ligands despite the absence of a

B–H resonance in the ^1H NMR spectrum. Heteronuclear NMR shifts have previously been shown to be indicators of the oxidation state at uranium.³⁷ The ^{11}B resonance for **2-AzBz** is shifted significantly upfield of previously characterized uranium(III) complexes including Tp^*UEPh (E = O, S, Se, Te; ^{11}B : -1.2 – 0.1 ppm),³⁸ $\text{TpUI}_2(\text{THF})_3$ (15.7 ppm),³³ Tp^*UF (-7.8 ppm),³⁹ and $\text{Tp}^*\text{U}(2,2'\text{-bpy})$ (**1b**) (-27.14 ppm). Instead, the ^{11}B chemical shift for **2-AzBz** resembles that of Tp^*UF_2 (-63.7 ppm),³⁹ signifying formation of a uranium(IV) product. **2-AzBz** was also formed by treating **1b** with azobenzene with the expulsion of neutral 2,2'-bipyridine (details in Supporting Information).

Structural confirmation of **2-AzBz** was achieved by the analysis of single, X-ray quality crystals obtained from a concentrated THF solution stored at -35°C . Refinement of the data revealed an eight coordinate uranium bis(Tp^*) species bound by an η^2 -1,2-diphenylhydrazido moiety (Figure 1, left).

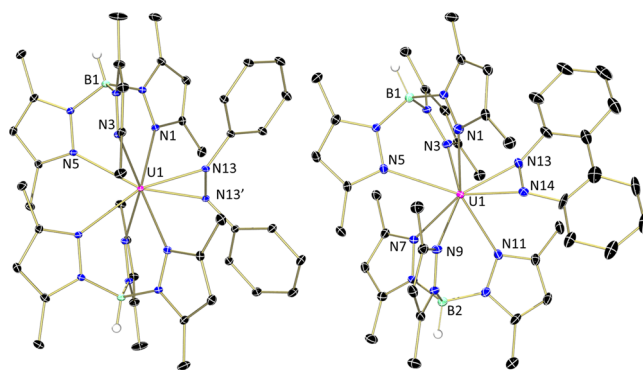


Figure 1. Molecular structures of **2-AzBz** (left) and **2-BCC** (right) displayed with 30% probability ellipsoids. Select hydrogen atoms and cocrystallized solvents have been omitted for clarity. Selected bond lengths for **2-AzBz**: U1–N13 = 2.2254(15); N13–N13' = 1.440(3) Å. For **2-BCC**: U1–N13 = 2.213(6); U1–N14 = 2.203(5); N13–N44 = 1.400(8) Å.

The U–N_{pyrazole} distances range from 2.518(6) to 2.654(7) Å and are unremarkable. The uranium–nitrogen distances of the η^2 -1,2-diphenylhydrazido are significantly shorter (U1–N13 = 2.2254(15) Å), suggesting a dianionic ligand. A two-electron-reduced azobenzene is further evinced by significant elongation of the diazo moiety (N13–N13' = 1.440(3) Å) compared to neutral *cis*-azobenzene (1.251 Å) and related *trans*-isomers.⁴⁰ The reduction of the N–N bond in **2-AzBz** is comparable to those observed in transition metal and lanthanide complexes bearing an (η^2 -1,2-RNNR)²⁻ unit, including $\text{Cp}^*\text{WMe}_3(\eta^2\text{-MeNNMe})$ (1.38(1) Å),⁴¹ $\text{Cp}_2\text{Zr}(\eta^2\text{-PhNNPh})(\text{NC}_5\text{H}_5)$ (1.434(4) Å),⁴² (κ^2 -(η^5 -C₅H₄SiMe₂)₂)Mo(η^2 -PhNNPh) (1.4061(9) Å),⁴³ [$\text{Cp}^*(\text{THF})\text{Sm}$]₂[N₂Ph₂]₂ (1.44(1) Å), and [$\text{Cp}_2(\text{THF})\text{Yb}$]₂[N₂Ph₂]₂ (1.470(6) Å).⁴⁴ Additionally, the N–N bond in **2-AzBz** is significantly more reduced than the analogous bond in [$((\text{SiMe}_2\text{NPh})_3\text{-tacn})\text{U}(\eta^2\text{-N}_2\text{Ph}_2)$] (1.353(4) Å)⁴⁵ and $\text{Cp}^*\text{Sm}(\text{N}_2\text{Ph}_2)(\text{THF})$ (1.388(15) Å),⁴⁴ both of which are characterized as containing a singly reduced, (PhNNPh)¹⁻, ligand. Moreover, the molecular structure of the azobenzene radical anion, [PhNNPh]¹⁻, has recently been determined, and the N–N distance of 1.331(17) Å is shorter than that observed in **2-AzBz**.⁴⁶

In the formation of **2-AzBz**, azobenzene is formally reduced by two electrons while both the uranium(III) center and the alkyl substituent of **1a** (or bipyridine of **1b**) are each oxidized

by a single electron. Cooperation between metal and ligand to afford substrate reduction by uranium(III) precursors **1a** and **1b** has previously been observed in this system in the formation of $\text{Tp}^*_2\text{U}(\text{NR})$ ($\text{R} = \text{Ph}, \text{Mes}, \text{Ad}$)³⁵ and $\text{Tp}^*_2\text{U}(\text{O})$.³⁴ Heating **2-AzBz** at 70 °C for several hours resulted in neither decomposition of the complex nor formation of the corresponding uranium(VI) bis(imido). This is in stark contrast to what had been observed in the bis(Cp^*) system, where a fleeting uranium(IV) η^2 -hydrazido intermediate, " $\text{Cp}^*_2\text{U}(\eta^2\text{-N}_2\text{Ph}_2)$ ", is proposed to undergo N–N bond cleavage at room temperature, suggesting that the U(IV) to U(VI) oxidation is facile.^{5,47}

The reactivities of complexes **1a** and **1b** toward benzo[*c*]-cinnoline were also investigated. This substrate presents interesting possibilities for reactivity because of the following: (1) the first reduction potential of benzo[*c*]cinnoline is significantly more negative than that of azobenzene (-2.084 vs -1.604 V), potentially preventing the two-electron reduction; (2) it is rigid, and the resultant reduced ligand would be planar, facilitating stabilization of a radical; or (3) the reaction may form a *cis*-bis(imido) analogous to $\text{Cp}^*_2\text{U}(\text{NPh})_2$ due to the tethered phenyl substituents.

Addition of benzo[*c*]cinnoline to a cold THF solution of **1a** (-35 °C) resulted in a gradual color change to dark red/purple over *ca.* 10 min (eq 1, left). Investigation of the crude mixture by ¹H NMR spectroscopy confirmed the formation of bibenzyl concomitant with consumption of benzo[*c*]cinnoline. Following workup, the spectrum revealed 14 paramagnetically shifted resonances ranging from -28.52 to 33.72 ppm allowing assignment as $\text{Tp}^*_2\text{U}(\text{BCC})$ (**2-BCC**, eq 1). Unlike **2-AzBz**, the B–H resonance was identified at -14.58 ppm with the corresponding ¹¹B resonance observed at -52.40 ppm, similarly upfield shifted and suggestive of uranium(IV). Slower reactivity was observed by addition of benzo[*c*]cinnoline to a toluene solution of **1b**, with the same color change noted to form **2-BCC** over 12 hours with expulsion of neutral 2,2'-bipyridine (synthetic details in Supporting Information).

For purposes of comparison to **2-AzBz**, single X-ray quality crystals of **2-BCC** obtained from a concentrated diethyl ether/THF (1:3) solution stored at -35 °C were analyzed by X-ray diffraction (Figure 1, right). Refinement of the data revealed the anticipated bis(Tp^*) uranium complex bound by an η^2 -benzo[*c*]cinnoline. The U–N_{BCC} distances (2.213(6) and 2.203(5) Å) are consistent with uranium(IV) anionic amide linkages and are nearly identical to those found in **2-AzBz** and the constrained-geometry organouranium catalyst, $(\text{Me}_2\text{Si}(\eta^5\text{-Me}_4\text{C}_5)(^t\text{BuN}))\text{U}(\text{NMe}_2)_2$ (2.207(4) and 2.212(4) Å).⁴⁸ Since metal-to-ligand backbonding is difficult for elements of the f-block,⁴⁹ N–N bond elongation is a useful metric to assess benzo[*c*]cinnoline reduction; in this case, the elongation of the N–N bond by *ca.* 0.09 Å, as compared to the free ligand (1.292(3) vs 1.400(8) Å),⁵⁰ is indicative of reduction. This distance in **2-BCC** is within error of the only other reported benzo[*c*]cinnoline f-block complex, $\text{Yb}(\text{BCC})_3(\text{THF})_2$. In this case, the three benzo[*c*]cinnoline ligands are characterized as monoanionic, consistent with a Yb^{3+} formulation by charge balance.⁵¹ In the case of **2-BCC**, additional spectroscopic data was obtained to determine the extent of reduction and uranium oxidation state.

Electronic absorption spectroscopy was employed to support the oxidation state of uranium in **2-AzBz** and **2-BCC** (Figure 2). For both species, data were obtained from 280 to 2100 nm in THF at ambient temperature. In the near-infrared region, 2-

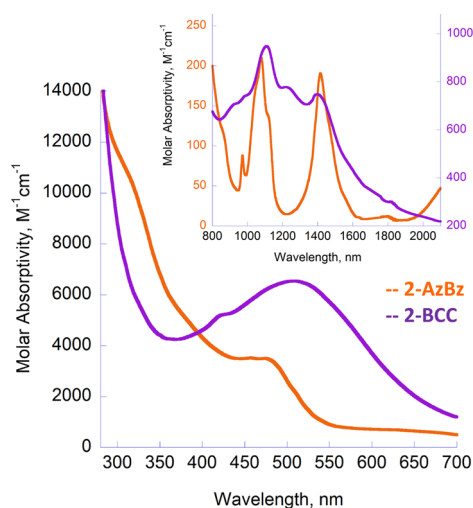


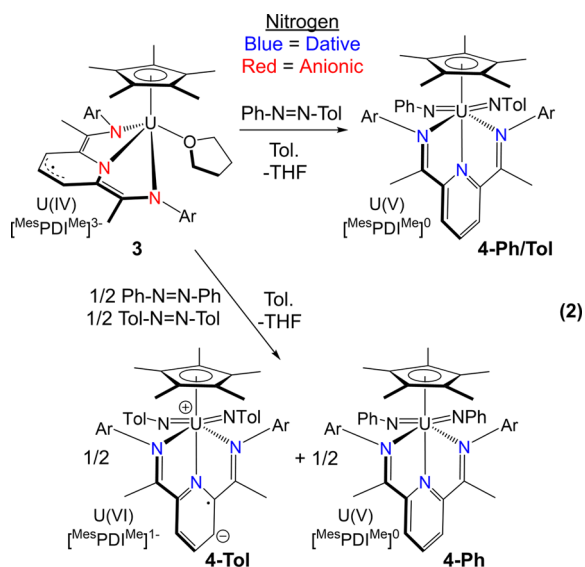
Figure 2. Electronic absorption spectra of **2-AzBz** (orange) and **2-BCC** (purple) recorded in THF at ambient temperature. Solvent overtones between 1670 and 1760 nm have been omitted for clarity.

AzBz displays a pair of sharp, weakly intense *f–f* transitions ($\lambda_{\text{max}} = 1416, 1078$ nm; $\epsilon = 191, 210$ $\text{M}^{-1} \text{cm}^{-1}$) consistent with a $5f^2$ complex (Figure 2, inset). These same transitions are observed in **2-BCC** ($\lambda_{\text{max}} = 1398, 1109$ nm) but are of much greater intensity and engulfed by an ill-defined broad transition throughout the region ($\epsilon \sim 600\text{--}900$ $\text{M}^{-1} \text{cm}^{-1}$). The visible region of **2-BCC** displays an intense color producing band at 509 nm ($\epsilon = 6540$ $\text{M}^{-1} \text{cm}^{-1}$) consistent with the deep red/purple color of the complex. In **2-AzBz**, this band appears as a weakened shoulder at 472 nm ($\epsilon = 3495$ $\text{M}^{-1} \text{cm}^{-1}$) consistent with the translucent yellow/brown appearance of the complex attributed to decreased conjugation of the η^2 -hydrazido ligand.

Thus, combining these electronic absorption spectroscopic data with our structural studies supports that both **2-AzBz** and **2-BCC** have dianionic diazene ligands and uranium(IV), $5f^2$ ions. We hypothesize that the observed double reduction of azobenzene and benzo[*c*]cinnoline is driven by attainment of the thermodynamically stable uranium(IV) oxidation state.

Pyridine(diimine) Complexes. With the general understanding obtained from **2-AzBz** and **2-BCC** of the intermediate η^2 -species in the four-electron diazene cleavage at uranium, we explored the same substrates with our highly reducing pyridine(diimine) system, since we have previously shown the ability of $\text{Cp}^*\text{U}(\text{MesPDI}^{\text{Me}})(\text{THF})$ (**3**) and $\text{Cp}^*\text{U}(^t\text{Bu-MesPDI}^{\text{Me}})(\text{THF})$ (**3-^tBu**) to cleave $\text{Ar-N}=\text{N-Ar}$ ($\text{Ar} = p\text{-Tol}, \text{Ph}$) to form bis(imido) species.^{17,19} While the isolation of complexes **2** would suggest this process occurs in a concerted fashion at a single metal center, the possibility of a bimetallic mechanism could not be discounted since this is often observed for f-block metals. For instance, Evans and co-workers have isolated a variety of Sm(III) complexes bearing bridging $[\text{PhN-NPh}]^{2-}$ units, including $\text{Cp}^*_2\text{Sm}(\mu\text{-PhNNPh})\text{-SmCp}^*_2$ ⁵² and $\text{Cp}^*(\text{THF})\text{Sm}(\mu\text{-}\eta^2\text{-}\eta^2\text{-PhNNPh})_2\text{SmCp}^*(\text{THF})$.⁴⁴

To distinguish between a mono- or bimetallic N–N bond cleavage pathway, a crossover experiment was performed by addition of a stoichiometric solution of $\text{Ph-N}=\text{N-Ph}$ and $\text{Tol-N}=\text{N-Tol}$ to **3** (eq 2, bottom). ¹H NMR spectroscopy of the crude reaction mixture revealed only the formation of $\text{Cp}^*\text{U}(\text{NPh})_2(\text{MesPDI}^{\text{Me}})$ (**4-Ph**) and $\text{Cp}^*\text{U}(\text{NTol})_2(\text{MesPDI}^{\text{Me}})$ (**4-Tol**) (as compared to literature). The crossover



product, $\text{Cp}^*\text{U}(\text{NPh})(\text{NTol})(\text{MesPDI}^{\text{Me}})$ (**4-Ph/Tol**, *vide infra*), was not detected, which is in contrast to the previous observation for the addition of two-electron oxidants to $[\text{Cp}^*\text{U}(\text{MesPDI}^{\text{Me}})]_2$ ($\text{Cp}^* = 7,7\text{-dimethylbenzylcyclopentadienide}$), where complexes of the type $\text{Cp}^*\text{U}(\text{EPh})_2(\text{MesPDI}^{\text{Me}})$ ($\text{E} = \text{S}, \text{Se}$) were obtained through radical oxidative addition.⁵³ Despite this result, **4-Ph** and **4-Tol** are known to exist in different electronic ground states, suggesting that the kinetics of addition may be different.¹⁹

As a further probe, the reactivity of **3** was tested with the mixed aryldiazene, $\text{PhN}=\text{NTol}$, resulting in an immediate darkening of the toluene solution (eq 2, top). Investigation of the crude mixture by ^1H NMR spectroscopy revealed neither **4-Ph** nor **4-Tol** but a new C_s symmetric, paramagnetic species, with 15 broadened resonances assigned as **4-Ph/Tol**. The electronic absorption spectrum of **4-Ph/Tol** displays a featureless visible region with two weakly intense absorbances at 1659 and 1615 nm (124 and $81 \text{ M}^{-1} \text{ cm}^{-1}$, respectively) consistent with a uranium(V) center (Figure S8)⁵⁴ and, by charge balance considerations, a neutral pyridine(diimine) similar to **4-Ph**.¹⁷

Structural confirmation of **4-Ph/Tol** was achieved by analysis of single, X-ray quality crystals obtained from a concentrated diethyl ether solution stored at $-35 \text{ }^\circ\text{C}$ (Figure 3, Table 1). Refinement of the data revealed two independent molecules per unit cell. As each have statistically indistinguishable bond

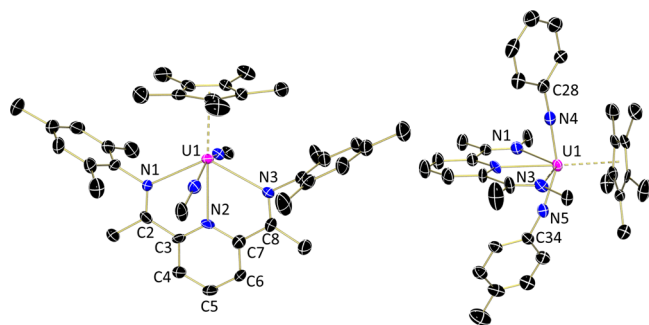
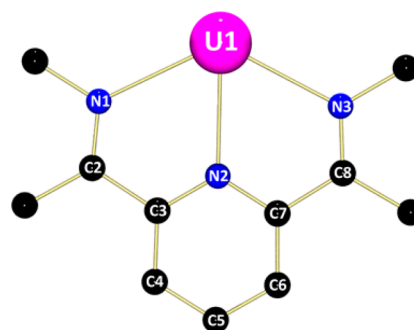


Figure 3. Molecular structure of **4-Ph/Tol** displayed with 30% probability ellipsoids. Hydrogen atoms, solvent molecules, select aryl (left) and 2,4,6-trimethylphenyl (right) substituents, and a second molecule in the unit cell have been omitted for clarity.

Table 1. Structural Parameters of **4-Ph/Tol**, **5**, **6**, and **7** with Pyridine(diimine) Numbering Scheme Depicted Here

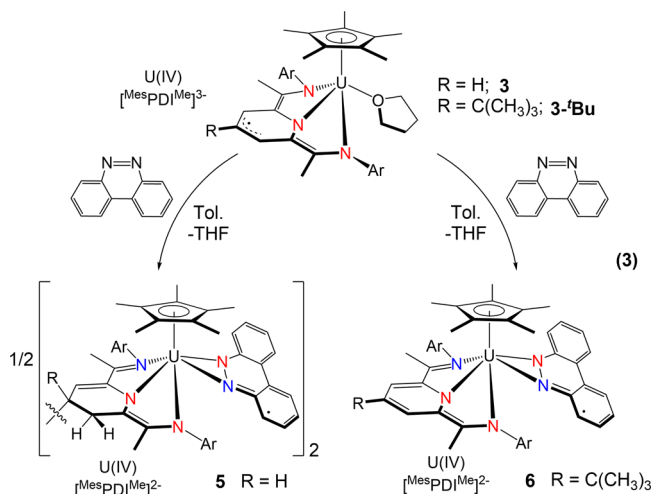


bond (Å)	4-Ph/Tol	5	6	7
U1–N1	2.619(6)	2.811(4)	2.382(6)	2.612(10)
U1–N2	2.594(6)	2.238(4)	2.344(6)	2.258(9)
U1–N3	2.587(7)	2.256(4)	2.349(6)	2.290(8)
U1–N4	2.010(7)	2.385(4)	2.369(6)	2.413(9)
U1–N5	2.005(7)	2.393(4)	2.367(6)	2.388(9)
U1–Ct	2.592	2.526	2.532	2.523
N1–C2	1.287(11)	1.296(6)	1.382(12)	1.314(14)
C2–C3	1.479(12)	1.470(7)	1.383(10)	1.466(16)
C3–C4	1.392(12)	1.342(7)	1.43(3)	1.344(16)
C4–C5	1.378(13)	1.502(7)	1.389(15)	1.450(18)
C5–C6	1.381(13)	1.539(7)	1.466(16)	1.370(17)
C6–C7	1.379(13)	1.511(6)	1.52(2)	1.433(16)
C7–C8	1.473(14)	1.366(7)	1.379(10)	1.353(15)
N2–C3	1.296(10)	1.381(6)	1.352(11)	1.384(15)
N2–C7	1.365(12)	1.397(6)	1.365(9)	1.431(14)
N3–C8	1.296(11)	1.421(6)	1.390(9)	1.418(14)
N4–N5		1.369(5)	1.382(8)	1.372(13)

metrics, only one species will be discussed. The anticipated pseudo-octahedral uranium *trans*-bis(imido) ($\text{N4–U1–N5} = 154.8(3)^\circ$) complex capped by an $\eta^5\text{-Cp}^*$ ($\text{U1–Ct} = 2.592 \text{ \AA}$) was confirmed. Both the phenyl and tolyl(imido) substituents ($2.010(7)$ and $2.005(7) \text{ \AA}$, respectively) are similar to those observed in **4-Ph**, characterized as containing a uranium(V) ion.¹⁷ Due to steric pressure imparted on the imido substituents by the bulky Cp^* and subsequent disruption of the inverse *trans*-influence, the $\text{U}=\text{N}$ bond distances are slightly elongated as compared to other *trans*-bis(imido) uranium(V) complexes.⁵⁵ The long linkages to the pyridine(diimine) nitrogen atoms ($2.619(6)$, $2.594(6)$, $2.587(7) \text{ \AA}$) and aromaticity in the pyridine ring confirm a neutral chelate.

The four-electron cleavage to form **4-Ph/Tol** proceeds with three reducing electrons provided from the redox-active ligand and only a single equivalent from the metal center. Additionally, the observation of **4-Ph/Tol** as the only complex formed during the reaction suggests that this process occurs at a single uranium center with concerted diazene cleavage. These findings for uranium are consistent with those observed for its transition metal counterpart, tungsten. Rothwell and co-workers observed cleavage of $\text{PhN}=\text{NTol}$ at a single tungsten, $\text{W}(\text{OC}_6\text{HPh}_3\text{-}\eta^6\text{-C}_6\text{H}_5)(\text{OAr})(\text{PMe}_2\text{Ph})$ ($\text{OAr} = 2,3,5,6\text{-tetraphenylphenoxide}$), to form the mixed bis(imido), $(\text{ArO})_2\text{W}(\text{NTol})(\text{NPh})$.⁵⁶ In that case, the aryl(imido) substituents were found to gradually equilibrate to form the bis(tolyl) and bis(phenylimido) over days in solution. Such behavior was not observed for **4-Ph/Tol**; thus, formation of **4-Ph/Tol** further substantiates the hypothesis of Burns and co-workers for the cleavage of azobenzene by “ Cp^*_2U ” systems.¹²

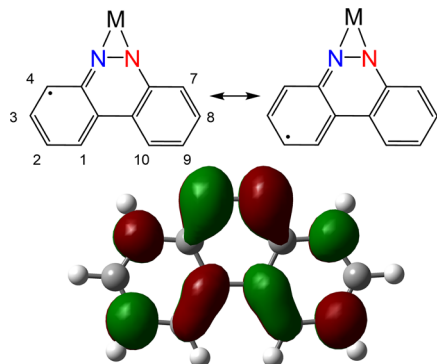
We envisioned the bis(imido) formation by **3** as an excellent opportunity to probe cooperative metal–ligand oxidation. We hypothesized that, by employing benzo[*c*]cinnoline, isolation of an intermediate η^2 -bound substrate would be possible because its tethered aryl rings would disallow full cleavage of the N–N bond to form a *trans*-bis(imido) as noted for PhN=NPh. Addition of a single equivalent of benzo[*c*]cinnoline to **3** in toluene produced an immediate reaction and isolation of a brown powder upon workup (eq 3, left). ^1H NMR



spectroscopic characterization revealed 21 paramagnetically shifted resonances ranging from -211.62 to 60.11 ppm consistent with asymmetry in the pyridine(diimine). The largest resonance, at 1.11 ppm, was assigned to the Cp* while the two furthest upfield (-211.62 and -153.27 ppm) and two furthest downfield (56.57 and 60.11 ppm) resonances were assigned to bound benzo[*c*]cinnoline. Far-shifted ^1H NMR resonances in **1b**, as well as in both dioxophenoxazine⁵⁷ and pyridine(diimine)²³ uranium derivatives, have previously been attributed to ligand radical character, suggesting a singly reduced η^2 -benzo[*c*]cinnoline (Scheme 2).

Analysis of single, brown crystals obtained from a concentrated THF solution layered with *n*-pentane at -35 °C by X-ray diffraction revealed a dimeric species, $[\text{Cp}^*\text{U}(\text{BCC})-(\text{MesHPDI}^{\text{Me}})]_2$ (**5**), after refinement (Figure 4, Table 1). Bound by an η^5 -Cp* (U1–Ct = 2.526 Å), the uranium center

Scheme 2. Relevant Resonance Forms of Singly Reduced Benzo[*c*]cinnoline^a and Free Ligand LUMO Depiction



^aNumbering convention included. Red = anionic nitrogen. Blue = neutral nitrogen.

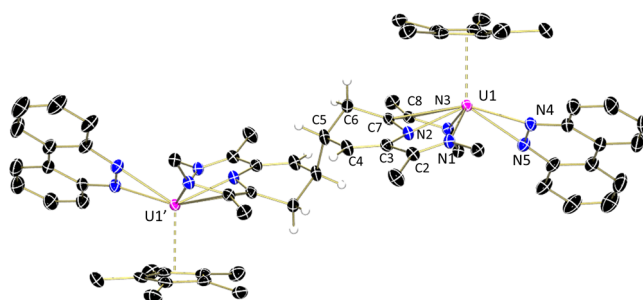


Figure 4. Molecular structure of **5** displayed with 30% probability ellipsoids. 2,4,6-Trimethylphenyl substituents, solvent molecules, and selected hydrogen atoms are omitted for clarity.

contains two short U–N_{PDI} contacts (U1–N2 = $2.238(4)$ Å; U1–N3 = $2.256(4)$ Å), one long contact (U1–N1 = $2.811(4)$ Å), and two intermediate bonds to the benzo[*c*]cinnoline (U1–N4 = $2.385(4)$ Å; U1–N5 = $2.393(4)$ Å). Reduction of the benzo[*c*]cinnoline N=N double bond is apparent by its elongation to $1.370(5)$ Å. The pyridine(diimine) intraligand distances are consistent with a closed shell dianionic ligand with alternating long and short distances, analogous to Cp*UI–(MesPDI^{Me}) (**3-I**). The C–N_{imine} distances vary widely between single (N3–C8 = $1.421(6)$ Å) and double bond (N1–C2 = $1.296(6)$ Å) character, while the adjacent C_{imine}–C_{pyridine} distances show the opposite character (C7–C8 = $1.366(7)$ Å; C2–C3 = $1.470(7)$ Å). This trend is broken as coupling at the *para*-pyridine (C5) occurs with concomitant H atom abstraction at the adjacent carbon (C6).

To rationalize the formation of **5**, the reaction was repeated in a variety of solvents with reproducible yields ranging from 60% to 80% after purification. Presumably, the one-electron oxidation of $[\text{MesPDI}^{\text{Me}}]^{3-}$ results in an unstable triplet diradical electronic structure for $[\text{MesPDI}^{\text{Me}}]^{2-}$ prior to rearrangement to the stable closed shell resonance form observed for **3-I**, Cp^pUI(MesPDI^{Me}), and (MesPDI^{Me})UI₂(THF)₂.⁵⁸ To test whether C–C coupling or H atom abstraction occurs first, the reaction was repeated in low concentration in neat 1,4-cyclohexadiene. Under these conditions, **5** was the only observable product, suggesting H atom abstraction occurs subsequent to C–C coupling. Therefore, in the formation of **5**, oxidation of $[\text{MesPDI}^{\text{Me}}]^{3-}$ to $[\text{MesPDI}^{\text{Me}}]^{2-}$ results in a ligand radical at the *para*-pyridine that couples to another molecule bearing the same radical. To our knowledge, this *para*-pyridine coupling is rarely observed for two pyridine(diimine) ligands; generally coupling to the *para*-pyridine of pyridine(diimine) complexes occurs from either alkyl^{59,60} or hydride⁶¹ migration from the metal center. *para*-Coupling of unsubstituted pyridine radicals has been observed by Holland and co-workers in $[(\text{CH}(\text{C}(\text{Me})\text{N}(\text{DIPP}))_2\text{Fe}(\text{pyr})(\text{pyr}))^{1-}]$, and this was later prevented through use of 4-*tert*-butylpyridine.⁶²

Despite the observed coupling, charge balance considerations less the dianionic pyridine(diimine) and Cp* anion would afford one of three electronic structures in **5**: U(III)/(BCC)⁰, U(IV)/(BCC)¹⁻, or U(V)/(BCC)²⁻. To support one of these possibilities, we sought to disallow coupling through the *para*-position in a fashion similar to that of Holland and co-workers by using the ^tBu–MesPDI^{Me} ligand. Adding an equivalent of benzo[*c*]cinnoline to previously reported Cp*U–(^tBu–MesPDI^{Me})(THF) (**3-tBu**) resulted in isolation of a brown powder upon workup (eq 3, right). Analysis of the product by ^1H NMR spectroscopy revealed 20 paramagnetically

shifted resonances ranging from -138.23 to 36.18 ppm with similar peak distribution and symmetry to **5**, leading to the assignment as $\text{Cp}^*\text{U}(\text{BCC})(t\text{-Bu-MesPDI}^{\text{Me}})$ (**6**). The largest resonance (4.22 ppm) was assigned to the Cp^* protons, and the benzo[*c*]cinnoline protons were readily assignable by their splitting patterns. The furthest upfield resonances (-138.23 and -112.48 ppm) were assigned to the 2,9-position (triplet) and 4,7-position (doublet), respectively, consistent with radical character (Scheme 2). The remaining, less shifted resonances, 36.18 and 34.23 ppm, were assigned to the 3,8-position (triplet) and 1,10-position (doublet).

To determine if the *tert*-butyl substituent in **6** halted dimerization as predicted, single, X-ray quality crystals obtained from a concentrated toluene/*n*-pentane solution (2:1) at -35 °C were analyzed by X-ray diffraction. Refinement of the data revealed the desired monomeric pentamethylcyclopentadienyl ($\text{U1-Ct} = 2.532$ Å) uranium pyridine(diimine) complex bound by an η^2 -benzo[*c*]cinnoline (Figure 5, Table 1). The uranium–

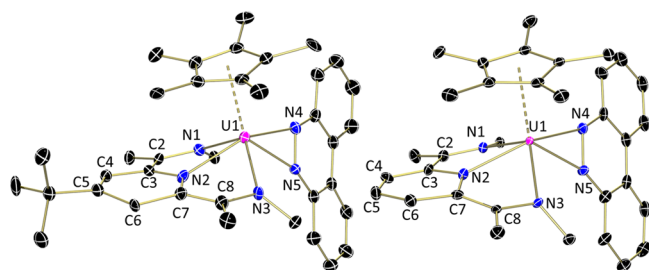
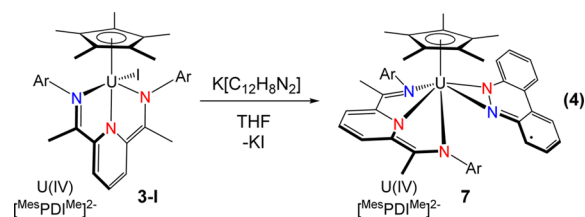


Figure 5. Molecular structures of **6** (left) and **7** (right) displayed with 30% probability ellipsoids. For 2,4,6-trimethylphenyl substituents, only the *ipso* carbon atoms are shown, and solvent molecules and hydrogen atoms have been omitted for clarity.

pyridine(diimine) distances ($\text{U1-N1} = 2.382(6)$ Å, $\text{U1-N2} = 2.344(6)$ Å, $\text{U1-N3} = 2.349(6)$ Å) are all shorter or within error of $(\text{MesPDI}^{\text{Me}})\text{U}(\text{THF})_2$,⁴⁷ suggesting a dianionic pyridine(diimine). Further, the C–N_{imine} ($\text{N1-C2} = 1.382(12)$, $\text{N3-C8} = 1.352(11)$ Å) bonds are elongated while the adjacent C_{imine}–C_{pyridine} ($\text{C2-C3} = 1.383(10)$, $\text{C7-C8} = 1.379(10)$ Å) bonds are contracted, both within the parameters set forth by Budzelaar and co-workers for dianionic pyridine(diimine) ligands.⁶³ Due to refined disorder in the *tert*-butyl and pyridine (C4-C5-C6), a detailed pyridine(diimine) intraligand bond distance discussion is not possible. Both uranium–benzo[*c*]cinnoline bonds are shorter than expected for only dative nitrogen interactions ($2.369(6)$ and $2.367(6)$ Å), while the diazo N4-N5 unit displays considerable reduction ($1.382(8)$ Å).

In the formation of **6**, the *para-tert*-butyl moiety prevents the dimerization brought about by an unstable intermediate electronic structure derived through single-electron oxidation of the reduced ligand. Electronic rearrangement affords a stable dianionic pyridine(diimine). As such, we hypothesized that a monomeric derivative of **5**, $\text{Cp}^*\text{U}(\text{BCC})(\text{MesPDI}^{\text{Me}})$ (**7**), should be attainable if a route other than $[\text{MesPDI}^{\text{Me}}]^{3-}$ oxidation is chosen. To test this hypothesis, we sought to synthesize **7** via salt metathesis rather than by a redox reaction as this would result in no net change in the electronic structure, removing the need for electronic rearrangement. To achieve this, *in situ* $\text{K}(\text{benzo}[c]\text{cinnoline})$ was generated by reduction with potassium graphite and added to an equivalent of $\text{Cp}^*\text{U}(\text{MesPDI}^{\text{Me}})$ (**3-I**) (eq 4). After workup, the isolated



dark brown/green complex was analyzed by ^1H NMR spectroscopy revealing a paramagnetic spectrum with similar peak distributions to **5** and **6** with the largest resonance assigned to the Cp^* (1.95 ppm). Again, the furthest downfield (62.73 and 60.89 ppm) and upfield (-216.46 and -158.04 ppm) resonances correspond to bound benzo[*c*]cinnoline bearing radical character allowing for assignment as $\text{Cp}^*\text{U}(\text{BCC})(\text{MesPDI}^{\text{Me}})$ (**7**).

Structural confirmation of monomeric **7** was achieved by X-ray diffraction analysis of crystals obtained from a concentrated hexamethyldisiloxane/*n*-pentane (1:5) solution stored at -35 °C. Refinement of the data revealed the monomeric analogue of **5**, a uranium pyridine(diimine) complex bound by an η^2 -benzo[*c*]cinnoline with an η^2 - Cp^* ($\text{U1-Ct} = 2.523$ Å) cap (Figure 5, Table 1). The η^2 -diazo interaction displays two uranium–nitrogen distances of intermediate length ($2.413(9)$ and $2.388(9)$ Å) consistent with a singly reduced moiety with the N–N bond reduced to $1.372(13)$ Å. The tridentate pyridine(diimine) chelate possesses the alternating long and short intraligand bond distances of a classic closed shell dianion. This electronic structure is further borne out by a single long uranium–nitrogen interaction ($\text{U1-N1} = 2.612(10)$ Å) as well as two short contacts ($\text{U1-N2} = 2.258(9)$ Å; $\text{U1-N3} = 2.290(8)$ Å).

To probe the existence of benzo[*c*]cinnoline radical character in complexes **5**–**7**, X-band EPR spectroscopy was employed (Figure 6). Each species displays a weakly intense, broadened isotropic signal centered at $|g| = 1.974$ at room temperature in toluene, similar to that observed for $\text{Cp}^*\text{UO}_2(\text{MesPDI}^{\text{Me}})$ ($|g| = 1.974$), which contains a pyridine(diimine) radical.¹⁸ Uranium–

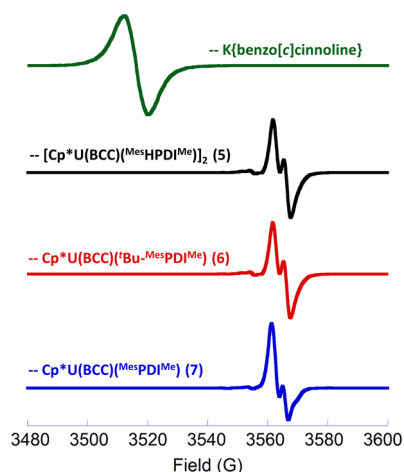


Figure 6. EPR spectra of *in situ* generated $\text{K}(\text{benzo}[c]\text{cinnoline})$ (green, toluene:THF 5:1, 6.81 mM, power 0.05 mW, modulation 0.01 mT/100 kHz), **5** (black, toluene, 2.63 mM, power 4.08 mW, modulation 0.10 mT/100 kHz), **6** (red, toluene, 7.00 mM, power 6.04 mW, modulation 0.15 mT/100 kHz), and **7** (blue, toluene, 4.96 mM, power 3.03 mW, modulation 0.40 mT/100 kHz) recorded at ambient temperature. Frequency: 9.85 GHz.

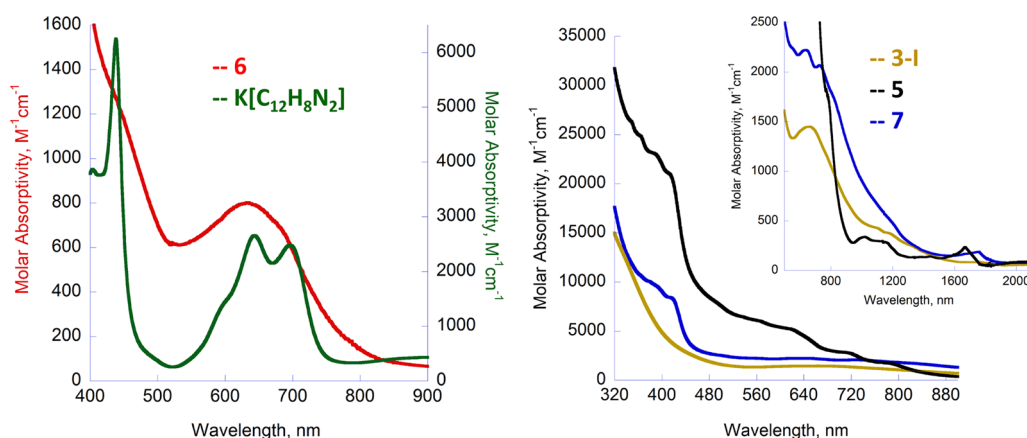


Figure 7. Electronic absorption spectra. Left: Complex **6** (red) and K(benzo[*c*]cinnoline) (green). Right: Complexes **3-I** (gold), **5** (black), and **7** (blue). All data were obtained in THF at ambient temperature. Solvent overtones between 1670 and 1760 nm have been omitted for clarity.

(III) and uranium(V) complexes are generally known to be EPR silent above liquid nitrogen temperatures,⁶⁴ while uranium $5f^2$ species are expected to produce an EPR signal at very low temperature only under rare circumstances,⁶⁵ suggesting the observed room temperature signals for **5–7** are ligand radical derived. Owing to the broadened signals, each displays a poorly resolved hyperfine splitting pattern consistent with previous studies on the spectroscopic investigations of the expected splitting pattern of the benzo[*c*]cinnoline radical anion.^{66–69} Although poorly resolved, the observed splitting is similar to that noted for the product from the room temperature chemical oxidation of $\text{UO}_2(\text{salophen}^{\text{tBu}})(\text{H}_2\text{O})$ (salophen^{tBu} = *N,N'*-bis(3,5-di-*tert*-butylsalicylidene)-1,2-phenylenediamine), which has been attributed to a radical cation localized on the salophen ligand.⁷⁰ The *g*-values of **5–7** are significantly shifted from that of *in situ* generated K(benzo[*c*]cinnoline) (Figure 6, green trace) ($|g| = 2.002$) and its derivatives⁷¹ suggesting that the ligand radicals are associated with uranium but not localized there.

To gain further insight into their electronic structures, complexes **5**, **6**, and **7** were investigated by electronic absorption spectroscopy (Figure 7). Data were recorded in THF at ambient temperature from 320 to 2100 nm. In the near-infrared region, each complex displays weakly intense absorptions characteristic of *f–f* transitions. These transitions are rather ill-defined and likely obscured by a visible band. For dimeric **5**, the visible region is composed of multiple transitions, while **6** possesses a defined absorbance at 635 nm ($802 \text{ M}^{-1} \text{ cm}^{-1}$). In **7**, this band appears at the same energy with emerging vibrational fine structure and is comparatively hyperchromic ($2222 \text{ M}^{-1} \text{ cm}^{-1}$). These visible bands are consistent with those observed in the electronic absorption spectrum of K(benzo[*c*]cinnoline) (Figure 7, left, green). For comparison, the spectrum of **3-I** was also obtained as this complex contains the same pyridine(diimine) electronic structure but does not contain the benzo[*c*]cinnoline ligand radical. For **3-I**, the same visible absorbance was observed at 664 nm ($\epsilon = 1550 \text{ M}^{-1} \text{ cm}^{-1}$). Therefore, this far visible absorbance for **5**, **6**, and **7** is attributable to contributions from both the closed shell pyridine(diimine) dianion as well as [benzo[*c*]cinnoline]¹⁻ while evidence of the benzo[*c*]cinnoline radical in complexes **5–7** appears as broad shoulders from 340 to 460 nm and are notably absent in **3-I**. The energies of these absorptions are similar to that observed in K(benzo[*c*]cinnoline) (438 nm, $6248 \text{ M}^{-1} \text{ cm}^{-1}$).

The magnetic properties of the pyridine(diimine) uranium species **3-I**, **5**, and **7** were measured in the solid state using SQUID magnetometry. Compound **3-I** was used as a reference, since this species was previously established to be a closed shell, uranium(IV) compound with no ligand radical(s) present.²³ The magnetic susceptibility for **3-I** ranges from $1.20 \text{ cm}^3 \text{ K/mol}$ (μ_{eff} value = 3.15) at 300 K to $0.03 \text{ cm}^3 \text{ K/mol}$ (μ_{eff} value = 0.46) at 2 K; the monotonic decrease in $\chi_{\text{M}}T$ values is typically encountered for noninteracting U(IV) ions, where ground state singlets show paramagnetic responses at higher temperatures due to population of magnetic excited states (Figure 8a).^{72–76} Furthermore, the magnetization of **3-I** is $0.07 \mu_{\text{B}}$ at 1.8 K under an applied dc magnetic field of 50 kOe (Figure 8b), which further supports the assignment of a singlet ground state without the presence of a ligand radical. We attribute the nonzero magnetization value to a small population of paramagnetic excited states.

Compound **7** displays a room temperature magnetic susceptibility value of $1.29 \text{ cm}^3 \text{ K/mol}$ (μ_{eff} value = 3.21) where the $\chi_{\text{M}}T$ product decreases slowly over all temperatures until 4 K where the $\chi_{\text{M}}T$ value is $0.67 \text{ cm}^3 \text{ K/mol}$ (μ_{eff} value = 2.32). While the high temperature magnetic susceptibility value for **7** is indistinguishable from compound **3-I**, the far different temperature-dependent susceptibility suggests a distinct electronic structure. The low temperature $\chi_{\text{M}}T$ value of **7** is higher than reported for other U(IV) complexes where one ligand radical is present.^{77–79} Notwithstanding, the magnetization for **7** saturates at $1.06 \mu_{\text{B}}$ at 1.8 K under an applied dc magnetic field of 50 kOe, consistent with the presence of a ligand radical combined with some minor occupation of U(IV) excited states.⁴⁷ The magnetization value can be understood as the combination of what is expected for a noninteracting monoradical ($1 \mu_{\text{B}}$ for $S = 1/2$, $g = 2.00$) and a model U(IV) complex like **3-I** ($0.07 \mu_{\text{B}}$). These data are also consistent with a recently reported U(IV)–ligand radical complex, where its magnetization saturates at $\sim 1.1 \mu_{\text{B}}$ at 0.33 K under an applied field of 40 kOe.⁴⁵ This hypothesis is in agreement with our spectroscopic data, which suggest that the ligand radical is isolated on the BCC moiety but interacts weakly with the U(IV) center.

Whereas the 300 K $\chi_{\text{M}}T$ value for compound **5** of $2.48 \text{ cm}^3 \text{ K/mol}$ (μ_{eff} value = 4.45) is comparable to $\chi_{\text{M}}T$ for **3-I** and **7** on a per-U atom basis, this value does not trend toward zero as the temperature is decreased. Instead, it decreases gradually to $1.10 \text{ cm}^3 \text{ K/mol}$ (μ_{eff} value = 2.97) at 7 K, whereupon the value

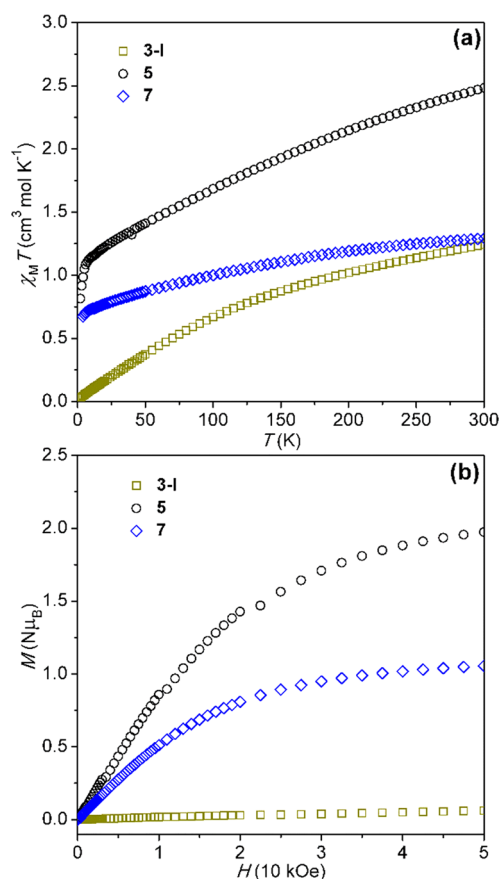


Figure 8. Top: Temperature dependence of magnetic susceptibilities for compounds 3-I (gold), 5 (black), and 7 (blue) obtained at an applied dc field of 5000 Oe. Bottom: Field dependence of magnetization for compounds 3-I, 5, and 7, collected at 1.8 K.

decreases more sharply to $0.82 \text{ cm}^3 \text{ K/mol}$ (μ_{eff} value = 2.56) at 2 K. The field dependence of magnetization, collected at 1.8 K, approaches (but does not reach) saturation at 50 kOe with a value of $1.99 \mu_B$ (Figure 8b), consistent with two unpaired electrons in the ground state and magnetic anisotropy. On the basis of the lack of substantial exchange interactions between $\text{BCC}^{\bullet-}$ and U(IV) observed in the related mononuclear compound 7 and the orbital singlet ground state observed for the U(IV) complex in 3-I, we can rationalize the low temperature susceptibility and magnetization properties of dimeric 7 as an $S = 1$ ground state resulting from ferromagnetic coupling of the ligand radical spins. Quantification of the exchange coupling is hampered by the presence of U(IV) ions, but susceptibility data corrected for the behavior of the “simple” U(IV) complex 3-I support the formulation of a triplet ground state (Figure S26 and further discussion in the SI). Here, the U(IV) ions do not substantially impact the exchange coupling, but may contribute to anisotropy through excited state contributions to the overall complex electronic structure. The expected magnetic anisotropy is observed as nonoverlapping isofield magnetization values as a function of reduced field (Figure S22). In addition, some frequency dependence in the out-of-phase susceptibility values (Figure S23) is observed, consistent with some involvement of the U(IV) centers.

In support of this assignment, we note that a diiron complex bridged by a dimerized dianionic (bi)pyridine ligand has been reported by Holland, Neese, and co-workers to show weak ferromagnetic coupling of the iron–ligand spin systems.⁶² In

the current work, the coupling in 5 appears to be qualitatively stronger (Figure S26) even though the bridging ligand in 5 is less conjugated than the dimerized pyridine species in the Holland/Neese report; we note that the C_i symmetry of 5 and two sp^3 hybridized bridge atoms leads to strict orthogonality of the π -based spin systems, whereas C_2 symmetry of the iron dimer might allow more orbital overlap and thus competing antiferromagnetic interactions. Conceptually related, another dinuclear species recently reported by Heyduk and some of us shows four spin centers (two ligand radicals and two iron centers) present in a molecule where the magnetic behavior was best modeled as two metal–ligand spin systems interacting ferromagnetically with magnetic anisotropy present.⁸⁰

Therefore, in our view the most reasonable representation of the magnetic data (and electronic structure) for compound 5 comprises two uranium–ligand coupled spin systems, each having one ligand radical (delocalized on the BCC ligand) and one U(IV) ion, the ferromagnetic coupling of which results in an $S = 1$ ground state. Overall, the electronic structures observed for compounds 5, 6, and 7, where each pyridine(diimine) is dianionic and each BCC fragment is monoanionic, derive from the driving force to attain the thermodynamically stable uranium(IV) oxidation state.

CONCLUSION

In summary, we have provided further examples of diazene activation by electron-rich uranium compounds; activation that depends both on the nature of the uranium framework and the diazene ligand. In the case of the bis- Tp^* system, isolation of the first dianionic η^2 -1,2-diphenylhydrazido ligand bound to uranium was possible, likely due to the steric protection of the bulky hydrotris(3,5-dimethylpyrazolyl)borate ligands. Significantly, the diazene has been reduced by two electrons, as $\text{Tp}^*_2\text{UCh}_2\text{Ph}$ acts as a source of divalent $[\text{Tp}^*_2\text{U}]$. In the case of the pyridine(diimine) system, complete N–N cleavage was noted and is attributed to both the relatively coordinatively unsaturated uranium center, and to the highly reducing trianionic pyridine(diimine) ligand that mediates a four-electron transfer for bond scission. Only in the case of the tethered diazene, benzo[*c*]cinnoline, is the N–N bond retained in this ligand system, and in each case, the presence of ligand radicals is supported by spectroscopic, structural, and magnetic studies.

The studies presented herein highlight the importance of ligand framework choice, in that utilizing the sterically demanding Tp^* permits isolation of the first uranium η^2 -1,2-diphenylhydrazido species. Thus, 2-AzBz serves as a model for this key intermediate proposed to be significant in N–N bond cleavage pathways, providing further evidence for Burns’ idea that four-electron diazene cleavage by uranium occurs at a single metal center. This idea was further substantiated using the highly reduced $\text{Cp}^*/\text{MesPDI}^{\text{Me}}$ system, where formation of the mixed *p*-tolyl/phenyl bis(imido) (4-Ph/Tol) was possible via cleavage of the asymmetric diazene $\text{PhN}=\text{NTol}$. Significantly, activation of benzo[*c*]cinnoline demonstrated that the first reduction of the diazo moiety occurs via oxidation of the pyridine(diimine) ligand, rather than uranium, maintaining the +4 metal oxidation state. Furthermore, products 5, 6, and 7 are an unusual family where both the pyridine(diimine) and benzo[*c*]cinnoline ligands house radicals simultaneously, although those present in $[\text{MesPDI}^{\text{Me}}]^{2-}$ are best described as a closed shell configuration. With this insight into the mechanism of diazene cleavage, further studies for the

synthesis of heteroleptic bis(imido) species from directed activation of N–N bonds are warranted and currently underway in our laboratory.

■ ASSOCIATED CONTENT

● Supporting Information

The Supporting Information is available free of charge on the ACS Publications website at DOI: 10.1021/acs.inorgchem.6b01922.

Crystallographic details for **6** (CIF)

Crystallographic details for **2-BCC** (CIF)

Crystallographic details for **7** (CIF)

Crystallographic details for **2-AzBz** (sample 1) (CIF)

Crystallographic details for **4-Ph/Tol** (CIF)

Crystallographic details for **5** (CIF)

Crystallographic details for **2-AzBz** (sample 2) (CIF)

NMR, electronic absorption, magnetic, and crystallographic data (PDF)

■ AUTHOR INFORMATION

Corresponding Author

*E-mail: sbart@purdue.edu.

Notes

The authors declare no competing financial interest.

■ ACKNOWLEDGMENTS

The authors acknowledge support from the Division of Chemical Sciences, Geosciences, and Biosciences, Office of Basic Energy Sciences, Heavy Elements Chemistry Program of the U.S. Department of Energy through Grant DE-SC0008479 (S.C.B., pyridine(diimine) work) and from the National Science Foundation (CAREER grant to S.C.B., CHE-1149875, Tp*₂U(III) alkyl work). M.P.S. and R.F.H. thank NSF (CHE-1363274) for support of magnetometry measurements at Colorado State University. S.C.B., M.Z., and J.J.K. thank Illinois State University's Prof. Christopher Hamaker and Prof. Gregory Ferrence for access to their ApexII diffractometer (funded by NSF-CHE Grant 1039689) for analysis of **2-AzBz**.

■ REFERENCES

- (1) Jia, H.-P.; Quadrelli, E. A. Mechanistic Aspects of Dinitrogen Cleavage and Hydrogenation to Produce Ammonia in Catalysis and Organometallic Chemistry: Relevance of Metal Hydride Bonds and Dihydrogen. *Chem. Soc. Rev.* **2014**, *43*, 547–564.
- (2) Pool, J. A.; Lobkovsky, E.; Chirik, P. J. Hydrogenation and Cleavage of Dinitrogen to Ammonia with a Zirconium Complex. *Nature* **2004**, *427*, 527–530.
- (3) Bernskoetter, W. H.; Lobkovsky, E.; Chirik, P. J. Kinetics and Mechanism of N₂ Hydrogenation in Bis(Cyclopentadienyl) Zirconium Complexes and Dinitrogen Functionalization by 1,2-Addition of a Saturated C–H Bond. *J. Am. Chem. Soc.* **2005**, *127*, 14051–14061.
- (4) Fox, A. R.; Bart, S. C.; Meyer, K.; Cummins, C. C. Towards Uranium Catalysts. *Nature* **2008**, *455*, 341–349.
- (5) Arney, D. S. J.; Burns, C. J.; Smith, D. C. Synthesis and Structure of the First Uranium(VI) Organometallic Complex. *J. Am. Chem. Soc.* **1992**, *114*, 10068–9.
- (6) MacDonald, M. R.; Fieser, M. E.; Bates, J. E.; Ziller, J. W.; Furche, F.; Evans, W. J. Identification of the + 2 Oxidation State for Uranium in a Crystalline Molecular Complex, [K(2.2.2-Cryptand)]-[(C₅H₄SiMe₃)₃U]. *J. Am. Chem. Soc.* **2013**, *135*, 13310–13313.
- (7) La Pierre, H. S.; Scheurer, A.; Heinemann, F. W.; Hieringer, W.; Meyer, K. Synthesis and Characterization of a Uranium(II) Monoarene Complex Supported by Δ Backbonding. *Angew. Chem., Int. Ed.* **2014**, *53*, 7158–7162.
- (8) Evans, W. J.; Nyce, G. W.; Ziller, J. W. Formal Three-Electron Reduction by an F-Element Complex: Formation of [((C₅Me₅)-(C₈H₈)U)₂(C₈H₈)] from Cyclooctatetraene and [(C₅Me₅)₃U]. *Angew. Chem., Int. Ed.* **2000**, *39*, 240–242.
- (9) Evans, W. J.; Kozimor, S. A.; Ziller, J. W.; Kaltsoyannis, N. Structure, Reactivity, and Density Functional Theory Analysis of the Six-Electron Reductant, [(C₅Me₅)₂U](μ-η⁶:η⁶-C₆H₆), Synthesized Via a New Mode of (C₅Me₅)₃M Reactivity. *J. Am. Chem. Soc.* **2004**, *126*, 14533–14547.
- (10) Evans, W. J.; Kozimor, S. A.; Ziller, J. W. [(C₅Me₅)₂U](μ-Ph)₂BPh₂] as a Four Electron Reductant. *Chem. Commun.* **2005**, 4681–4683.
- (11) Evans, W. J.; Montalvo, E.; Kozimor, S. A.; Miller, K. A. Multi-Electron Reduction from Alkyl/Hydride Ligand Combinations in U⁴⁺ Complexes. *J. Am. Chem. Soc.* **2008**, *130*, 12258–12259.
- (12) Warner, B. P.; Scott, B. L.; Burns, C. J. A Simple Preparative Route to Bis(Imido)Uranium(VI) Complexes by the Direct Reductions of Diazenes and Azides. *Angew. Chem., Int. Ed.* **1998**, *37*, 959–960.
- (13) Arney, D. S. J.; Burns, C. J. Synthesis and Properties of High-Valent Organouranium Complexes Containing Terminal Organoimido and Oxo Functional Groups. A New Class of Organo-F-Element Complexes. *J. Am. Chem. Soc.* **1995**, *117*, 9448–9460.
- (14) Kiplinger, J. L.; Morris, D. E.; Scott, B. L.; Burns, C. J. Enhancing the Reactivity of Uranium(VI) Organoimido Complexes with Diazoalkanes. *Chem. Commun.* **2002**, 30–31.
- (15) Kiplinger, J. L.; John, K. D.; Morris, D. E.; Scott, B. L.; Burns, C. J. [(C₅Me₅)₂U(Me)(Otf)]₂: A New Reagent for Uranium Metallocene Chemistry. Preparation of the First Actinide Hydrazonato Complexes. *Organometallics* **2002**, *21*, 4306–4308.
- (16) Matson, E. M.; Fanwick, P. E.; Bart, S. C. Diazoalkane Reduction for the Synthesis of Uranium Hydrazonido Complexes. *Eur. J. Inorg. Chem.* **2012**, *2012*, 5471–5478.
- (17) Cladis, D. P.; Kiernicki, J. J.; Fanwick, P. E.; Bart, S. C. Multi-Electron Reduction Facilitated by a Trianionic Pyridine(diimine) Ligand. *Chem. Commun.* **2013**, *49*, 4169–4171.
- (18) Kiernicki, J. J.; Cladis, D. P.; Fanwick, P. E.; Zeller, M.; Bart, S. C. Synthesis, Characterization, and Stoichiometric U=O Bond Scission in Uranyl Species Supported by Pyridine(diimine) Ligand Radicals. *J. Am. Chem. Soc.* **2015**, *137*, 11115–11125.
- (19) Kiernicki, J. J.; Ferrier, M. G.; Pacheco, J. S. L.; La Pierre, H. S.; Stein, B. W.; Zeller, M.; Kozimor, S. A.; Bart, S. C. *J. Am. Chem. Soc.* **2016**, *138*, 13941.
- (20) Pangborn, A. B.; Giardello, M. A.; Grubbs, R. H.; Rosen, R. K.; Timmers, F. J. Safe and Convenient Procedure for Solvent Purification. *Organometallics* **1996**, *15*, 1518–1520.
- (21) Matson, E. M.; Forrest, W. P.; Fanwick, P. E.; Bart, S. C. Functionalization of Carbon Dioxide and Carbon Disulfide Using a Stable Uranium(III) Alkyl Complex. *J. Am. Chem. Soc.* **2011**, *133*, 4948–4954.
- (22) Kraft, S. J.; Fanwick, P. E.; Bart, S. C. Synthesis and Characterization of a Uranium(III) Complex Containing a Redox-Active 2,2'-Bipyridine Ligand. *Inorg. Chem.* **2010**, *49*, 1103–1110.
- (23) Kiernicki, J. J.; Newell, B. S.; Matson, E. M.; Anderson, N. H.; Fanwick, P. E.; Shores, M. P.; Bart, S. C. Multielectron C–O Bond Activation Mediated by a Family of Reduced Uranium Complexes. *Inorg. Chem.* **2014**, *53*, 3730–3741.
- (24) Zhang, C.; Jiao, N. Copper-Catalyzed Aerobic Oxidative Dehydrogenative Coupling of Anilines Leading to Aromatic Azo Compounds Using Dioxygen as an Oxidant. *Angew. Chem.* **2010**, *122*, 6310–6313.
- (25) Kaiser, M.; Leitner, S. P.; Hirtenlehner, C.; List, M.; Gerisch, A.; Monkowius, U. Azobenzene-Functionalized N-Heterocyclic Carbenes as Photochromic Ligands in Silver(I) and Gold(I) Complexes. *Dalton Trans.* **2013**, *42*, 14749–14756.
- (26) Dennington, R.; Keith, T.; Millam, J. *Gaussview 5, 5.0.8*; Semicem Inc.: Shawnee Mission, KS, 2009.
- (27) *Bruker Advanced X-Ray Solutions, 2014.7-1*; Bruker AXS Inc.: Madison, WI, 2014.

- (28) Sheldrick, G. M. *Acta Crystallogr., Sect. A: Found. Crystallogr.* **2008**, *A64*, 112–122.
- (29) *SHELXTL*, 6.14; Bruker AXS Inc.: Madison, WI, 2000–2003.
- (30) Sheldrick, G. M. Crystal Structure Refinement with Shelxl. *Acta Crystallogr., Sect. A: Found. Adv.* **2015**, *71*, 3–8.
- (31) Huebschle, C. B.; Sheldrick, G. M.; Dittrich, B. Shelxle: A Qt Graphical User Interface for Shelxl. *J. Appl. Crystallogr.* **2011**, *44*, 1281–1284.
- (32) Bain, G. A.; Berry, J. F. Diamagnetic Corrections and Pascal's Constants. *J. Chem. Educ.* **2008**, *85*, 532.
- (33) Matson, E. M.; Kiernicki, J. J.; Fanwick, P. E.; Bart, S. C. Expanding the Family of Uranium(III) Alkyls: Synthesis and Characterization of Mixed-Ligand Derivatives. *Eur. J. Inorg. Chem.* **2016**, *2016*, 2527–2533.
- (34) Kraft, S. J.; Walensky, J.; Fanwick, P. E.; Hall, M. B.; Bart, S. C. Crystallographic Evidence of a Base-Free Uranium(IV) Terminal Oxo Species. *Inorg. Chem.* **2010**, *49*, 7620–7622.
- (35) Matson, E. M.; Crestani, M. G.; Fanwick, P. E.; Bart, S. C. Synthesis of U(IV) Imidos from $\text{Tp}^*_2\text{U}(\text{CH}_2\text{Ph})$ ($\text{Tp}^* = \text{Hydrotris}(3,5\text{-dimethylpyrazolyl})\text{borate}$) by Extrusion of Bibenzyl. *Dalton Trans.* **2012**, *41*, 7952–7958.
- (36) Matson, E. M.; Goshert, M. D.; Kiernicki, J. J.; Newell, B. S.; Fanwick, P. E.; Shores, M. P.; Walensky, J. R.; Bart, S. C. Synthesis of Terminal Uranium(IV) Disulfido and Diselenido Compounds by Activation of Elemental Sulfur and Selenium. *Chem. - Eur. J.* **2013**, *19*, 16176–16180.
- (37) Windorff, C. J.; Evans, W. J. ^{29}Si NMR Spectra of Silicon-Containing Uranium Complexes. *Organometallics* **2014**, *33*, 3786–3791.
- (38) Matson, E. M.; Breshears, A. T.; Kiernicki, J. J.; Newell, B. S.; Fanwick, P. E.; Shores, M. P.; Walensky, J. R.; Bart, S. C. Trivalent Uranium Phenylchalcogenide Complexes: Exploring the Bonding and Reactivity with CS_2 in the Tp^*_2UEPh Series (E = O, S, Se, Te). *Inorg. Chem.* **2014**, *53*, 12977–12985.
- (39) Clark, C. L.; Lockhart, J. J.; Fanwick, P. E.; Bart, S. C. Synthesis of Low-Valent Uranium Fluorides by C-F Bond Activation. *Chem. Commun.* **2015**, *51*, 14084–14087.
- (40) Mostad, A.; Roemming, C.; et al. Refinement of the Crystal Structure of *cis*-Azobenzene. *Acta Chem. Scand.* **1971**, *25*, 3561–3568.
- (41) Glassman, T. E.; Vale, M. G.; Schrock, R. R. Synthesis and Structure of a Tungsten(IV) η^2 -Dimethyldiazene Complex in Which the Diazene Ligand Behaves as a Four-Electron Donor. *Inorg. Chem.* **1992**, *31*, 1985–1986.
- (42) Walsh, P. J.; Hollander, F. J.; Bergman, R. G. Insertion of Alkynes into Zirconium-Nitrogen Bonds Leading to 2,3-Diazametallacyclopentenes. Generation and Reactivity of $\text{Cp}_2\text{Zr}(\text{N}_2\text{Ph}_2)$. *J. Organomet. Chem.* **1992**, *428*, 13–47.
- (43) Arnold, T.; Braunschweig, H.; Gross, M.; Kaupp, M.; Mueller, R.; Radacki, K. Electronic Structure and Reactivity of a [1], [1]Disilamolybdenocenophane. *Chem. - Eur. J.* **2010**, *16*, 3014–3020.
- (44) Evans, W. J.; Drummond, D. K.; Chamberlain, L. R.; Doedens, R. J.; Bott, S. G.; Zhang, H.; Atwood, J. L. Synthetic, Structural, and Reactivity Studies of the Reduction and Carbon Monoxide Derivatization of Azobenzene Mediated by Divalent Lanthanide Complexes. *J. Am. Chem. Soc.* **1988**, *110*, 4983–4994.
- (45) Antunes, M. A.; Coutinho, J. T.; Santos, I. C.; Marcalo, J.; Almeida, M.; Baldovi, J. J.; Pereira, L. C. J.; Gaita-Arino, A.; Coronado, E. A Mononuclear Uranium(IV) Single-Molecule Magnet with an Azobenzene Radical Ligand. *Chem. - Eur. J.* **2015**, *21*, 17817–17826.
- (46) Andrez, J.; Pécaut, J.; Bayle, P.-A.; Mazzanti, M. Tuning Lanthanide Reactivity Towards Small Molecules with Electron-Rich Siloxide Ligands. *Angew. Chem., Int. Ed.* **2014**, *53*, 10448–10452.
- (47) Anderson, N. H.; Odoh, S. O.; Yao, Y.; Williams, U. J.; Schaefer, B. A.; Kiernicki, J. J.; Lewis, A. J.; Goshert, M. D.; Fanwick, P. E.; Schelter, E. J.; Walensky, J. R.; Gagliardi, L.; Bart, S. C. Harnessing Redox Activity for the Formation of Uranium Tris(Imido) Compounds. *Nat. Chem.* **2014**, *6*, 919–926.
- (48) Stubbert, B. D.; Stern, C. L.; Marks, T. J. Synthesis and Catalytic Characteristics of Novel Constrained-Geometry Organoactinide Catalysts. The First Example of Actinide-Mediated Intramolecular Hydroamination. *Organometallics* **2003**, *22*, 4836–4838.
- (49) Kaltoyannis, N.; Scott, P. *The F Elements*; Oxford University Press: New York, 1999; p 85.
- (50) van der Meer, H. The Crystal Structure of 9,10-Diazaphenanthrene. *Acta Crystallogr., Sect. B: Struct. Crystallogr. Cryst. Chem.* **1972**, *B28*, 367–370.
- (51) Nakayama, Y.; Nakamura, A.; Mashima, K. Lanthanoid Complexes of Azobenzene and Benzo[C]Cinnoline Derived from Metallic Lanthanoids: Crystal Structures of Binuclear $[\text{SmI}(\text{THF})_3(\mu\text{-}\eta^2\text{-}\eta^2\text{-trans-PhNNPh})_2\text{SmI}(\text{THF})_3]$ and Mononuclear $[\text{Yb}(\text{Benzo}[c]\text{-cinnoline})_3(\text{THF})_2]$. *Chem. Lett.* **1997**, *26*, 803–804.
- (52) Evans, W. J.; Drummond, D. K.; Bott, S. G.; Atwood, J. L. Reductive Distortion of Azobenzene by an Organosamarium(II) Reagent to Form $[(\text{C}_5\text{Me}_5)_2\text{Sm}(\text{C}_6\text{H}_5)_2]^{2-}$: An X-ray Crystallographic Snapshot of an Agostic Hydrogen Complex on an *ortho*-Metalation Reaction Coordinate. *Organometallics* **1986**, *5*, 2389–2391.
- (53) Kiernicki, J. J.; Fanwick, P. E.; Bart, S. C. Utility of a Redox-Active Pyridine(diimine) Chelate in Facilitating Two Electron Oxidative Addition Chemistry at Uranium. *Chem. Commun.* **2014**, *50*, 8189–8192.
- (54) Lewis, A. J.; Mullane, K. C.; Nakamaru-Ogiso, E.; Carroll, P. J.; Schelter, E. J. The Inverse *Trans* Influence in a Family of Pentavalent Uranium Complexes. *Inorg. Chem.* **2014**, *53*, 6944–6953.
- (55) Jilek, R. E.; Spencer, L. P.; Lewis, R. A.; Scott, B. L.; Hayton, T. W.; Boncella, J. M. A Direct Route to Bis(Imido)Uranium(V) Halides via Metathesis of Uranium Tetrachloride. *J. Am. Chem. Soc.* **2012**, *134*, 9876–9878.
- (56) Lockwood, M. A.; Fanwick, P. E.; Eisenstein, O.; Rothwell, I. P. Mechanistic Studies of the Facile Four-Electron Reduction of Azobenzene at a Single Tungsten Metal Center. *J. Am. Chem. Soc.* **1996**, *118*, 2762–2763.
- (57) Pattenau, S. A.; Kuehner, C. S.; Dorfner, W. L.; Schelter, E. J.; Fanwick, P. E.; Bart, S. C. Spectroscopic and Structural Elucidation of Uranium Dioxophenoxazine Complexes. *Inorg. Chem.* **2015**, *54*, 6520–6527.
- (58) Anderson, N. H.; Odoh, S. O.; Williams, U. J.; Lewis, A. J.; Wagner, G. L.; Lezama Pacheco, J.; Kozimor, S. A.; Gagliardi, L.; Schelter, E. J.; Bart, S. C. Investigation of the Electronic Ground States for a Reduced Pyridine(diimine) Uranium Series: Evidence for a Ligand Tetraanion Stabilized by a Uranium Dimer. *J. Am. Chem. Soc.* **2015**, *137*, 4690–4700.
- (59) Sandoval, J. J.; Palma, P.; Alvarez, E.; Rodriguez-Delgado, A.; Campora, J. Dibenzyl and Diallyl 2,6-Bis(iminopyridine)zinc(II) Complexes: Selective Alkyl Migration to the Pyridine Ring Leads to Remarkably Stable Dihydropyridinates. *Chem. Commun.* **2013**, *49*, 6791–6793.
- (60) Sugiyama, H.; Aharonian, G.; Gambarotta, S.; Yap, G. P. A.; Budzelaar, P. H. M. Participation of the α,α' -Diiminopyridine Ligand System in Reduction of the Metal Center During Alkylation. *J. Am. Chem. Soc.* **2002**, *124*, 12268–12274.
- (61) Knijnenburg, Q.; Smits, J. M. M.; Budzelaar, P. H. M. Reaction of the Diimine Pyridine Ligand with Aluminum Alkyls: An Unexpectedly Complex Reaction. *Organometallics* **2006**, *25*, 1036–1046.
- (62) Dugan, T. R.; Bill, E.; MacLeod, K. C.; Christian, G. J.; Cowley, R. E.; Brennessel, W. W.; Ye, S.; Neese, F.; Holland, P. L. Reversible C–C Bond Formation between Redox-Active Pyridine Ligands in Iron Complexes. *J. Am. Chem. Soc.* **2012**, *134*, 20352–20364.
- (63) Knijnenburg, Q.; Gambarotta, S.; Budzelaar, P. H. M. Ligand-Centred Reactivity in Diiminepyridine Complexes. *Dalton Trans.* **2006**, 5442–5448.
- (64) Meyer, K.; Mindiola, D. J.; Baker, T. A.; Davis, W. M.; Cummins, C. C. Uranium Hexakisamido Complexes. *Angew. Chem., Int. Ed.* **2000**, *39*, 3063–3066.
- (65) Poole, C. P., Jr.; Farach, H. A. *Handbook of Electron Spin Resonance*; Springer-Verlag: New York, 1999; Vol. 2, p 660.
- (66) Strom, E. T.; Russell, G. A.; Konaka, R. Spin Densities in Azotype Radical Anions. *J. Chem. Phys.* **1965**, *42*, 2033–7.

(67) Chaudhuri, J.; Kume, S.; Jagur-Grodzinski, J.; Szwarc, M. Chemistry of Radical Anions of Heterocyclic Aromatics. I. Electron Spin Resonance and Electronic Spectra. *J. Am. Chem. Soc.* **1968**, *90*, 6421–5.

(68) Geske, D. H.; Padmanabhan, G. R. An Electron Spin Resonance Study of the Anion Radicals of 9,10-Diazaphenanthrene, 2,2'-Bipyrimidine, and 2,2'-Biisobenzimidazolylidene. *J. Am. Chem. Soc.* **1965**, *87*, 1651–5.

(69) Fujita, H.; Deguchi, Y.; Ohya-Nishiguchi, H.; Ishizu, K. Endor Study on the Anion Radical of Benzo[*c*]cinnoline. *Org. Magn. Reson.* **1981**, *16*, 245–6.

(70) Herasymchuk, K.; Chiang, L.; Hayes, C. E.; Brown, M. L.; Ovens, J.; Patrick, B. O.; Leznoff, D. B.; Storr, T. Synthesis and Electronic Structure Determination of Uranium(VI) Ligand Radical Complexes. *Dalton Trans.* **2016**, *45*, 12576–12586.

(71) Fischer, H.; Neugebauer, F. A.; Chandra, H.; Symons, M. C. R. Radical Cations and Anions of Benzo[*c*]cinnolines: An Electron Spin Resonance Study. *J. Chem. Soc., Perkin Trans. 2* **1989**, 727–30.

(72) Kindra, D. R.; Evans, W. J. Magnetic Susceptibility of Uranium Complexes. *Chem. Rev.* **2014**, *114*, 8865–8882.

(73) Castro-Rodriguez, I.; Meyer, K. Small Molecule Activation at Uranium Coordination Complexes: Control of Reactivity via Molecular Architecture. *Chem. Commun.* **2006**, 1353–1368.

(74) Schelter, E. J.; Veauthier, J. M.; Graves, C. R.; John, K. D.; Scott, B. L.; Thompson, J. D.; Pool-Davis-Tourneay, J. A.; Morris, D. E.; Kiplinger, J. L. 1,4-Dicyanobenzene as a Scaffold for the Preparation of Bimetallic Actinide Complexes Exhibiting Metal-Metal Communication. *Chem. - Eur. J.* **2008**, *14*, 7782–7790.

(75) Jilek, R. E.; Spencer, L. P.; Kuiper, D. L.; Scott, B. L.; Williams, U. J.; Kikkawa, J. M.; Schelter, E. J.; Boncella, J. M. A General and Modular Synthesis of Monoimidouranium(IV) Dihalides. *Inorg. Chem.* **2011**, *50*, 4235–4237.

(76) Schelter, E. J.; Wu, R.; Scott, B. L.; Thompson, J. D.; Cantat, T.; John, K. D.; Batista, E. R.; Morris, D. E.; Kiplinger, J. L. Actinide Redox-Active Ligand Complexes: Reversible Intramolecular Electron-Transfer in $U(Dpp-Bian)_2/U(Dpp-Bian)_2(THF)$. *Inorg. Chem.* **2010**, *49*, 924–933.

(77) Lam, O. P.; Feng, P. L.; Heinemann, F. W.; O'Connor, J. M.; Meyer, K. Charge-Separation in Uranium Diazomethane Complexes Leading to C-H Activation and Chemical Transformation. *J. Am. Chem. Soc.* **2008**, *130*, 2806–2816.

(78) Lam, O. P.; Anthon, C.; Heinemann, F. W.; O'Connor, J. M.; Meyer, K. Structural and Spectroscopic Characterization of a Charge-Separated Uranium Benzophenone Ketyl Radical Complex. *J. Am. Chem. Soc.* **2008**, *130*, 6567–6576.

(79) Castro-Rodriguez, I.; Nakai, H.; Zakharov, L. N.; Rheingold, A. L.; Meyer, K. A Linear, O-Coordinated η^1 -Co₂ Bound to Uranium. *Science* **2004**, *305*, 1757–1760.

(80) Wong, J. L.; Higgins, R. F.; Bhowmick, I.; Cao, D. X.; Szigethy, G.; Ziller, J. W.; Shores, M. P.; Heyduk, A. F. Bimetallic Iron-Iron and Iron-Zinc Complexes of the Redox-Active ONO Pincer Ligand. *Chem. Sci.* **2016**, *7*, 1594–1599.